Thermal-physics and energy performance of an innovative green roof system: The Cool-Green Roof

THERMAL-PHYSICS AND ENERGY PERFORMANCE OF AN INNOVATIVE GREEN ROOF SYSTEM: THE *COOL-GREEN ROOF*

Anna Laura Pisello[a,*], Cristina Piselli[a], Franco Cotana[a]
[a] Department of Engineering – University of Perugia, Via Duranti 67, 06125, Perugia, Italy
Tel. +39 075 585 3563, Email: *pisello@crbnet.it; piselli@crbnet.it; cotana@crbnet.it

ABSTRACT

Given the large amount of worldwide energy use associated with buildings' life cycle, in recent years various energy efficient strategies have been proposed to reduce buildings' environmental impact, e.g. green and cool roofs. The purpose of this work is to analyze an innovative type of green roof, named *Cool-Green roof* combining the features of both green and cool roofs. In fact, it is characterized by a specific vegetative layer able to optimize the quote of short-wave radiation reflected by the selected vegetation. After the analytical dissertation of the system, the developed solution is studied when applied in a case study building represented by a multifamily XVI century building in central Italy, characterized by cement based roof ceiling needing to be retrofitted. Both in-lab and in-field experimental analyses were carried out for evaluating the building thermal-physics and the solar reflectance and thermal emittance of the selected plant compared to other flat roof materials and greeneries. Additionally, the year-round performance of *Cool-Green roof* is assessed through calibrated and validated dynamic thermal-energy simulation. Main findings of the study show how the *Cool-Green roof* is able to reduce the number of indoor overheating hours in summer by 98.2%, with negligible penalties in winter, given its high insulation capability, typical of green roof solutions. Therefore, the *Cool-Green roof* could be considered as (i) a strategy for roof retrofitting in existing (even historic) buildings, as (ii) a solution for improving urban environment. Finally, the *Cool-Green Roof* could represent a promising mitigation strategy against urban heat island phenomenon, suitable for application even in those dense historical cities where other invasive mitigation techniques are unlikely applicable.

KEYWORDS

Cool Green Roof; Calibrated thermal-energy dynamic simulation; Energy efficiency in buildings; Urban Heat Island.

1. INTRODUCTION

The Energy Performance Building Directive 2010/31/EU (European Parliament and Council of the European Union, 2010) highlights that residential and commercial buildings account for a high rate, between 30% and 50%, of worldwide total annual energy consumption. Since the predicted average global air temperature rise of 2 °C represents a critical limit by 2030 and existing buildings are widely reported to operate inefficiently, the optimization of buildings' performance is a key issue to reduce global energy demand (IEA, 2009). Additionally, since the impressive increasing of the world population living in urban areas, which will reach about the 87% in 2050 in developed countries, the research issue to optimize energy efficiency of constructions located in urban areas is becoming increasingly urgent to address (Zinzi and Agnoli, 2012). The Italian context is peculiar from this point of view, since the majority of city centers are populated by historic buildings contributing to the local cultural heritage needing to be preserved (Pisello et al., 2013) and since national energy policies still neglect the urgent necessity to reduce building energy requirement for cooling (Zinzi et al., 2014). Therefore, specific architectural and physical constraints make the thermal-energy improvement of such buildings even more complicated to pursue.

In this panorama, new solutions for building roof systems in existing (even historic) or new buildings, such as green and cool roofs, play an important role in both increasing building energy performance and in mitigating local climate phenomena typical of dense urban contexts, such as Urban Heat Island (UHI) (Santamouris et al., 2011). In fact, roofs cover more than 20% of the total urban surface, and given the

limited green or free ground area in dense urban context (Santamouris, 2014) of historic city centers in particular, roof systems provide a suitable mean for the application of such mitigation techniques, also considering that UHI mitigation strategies themselves produce non-negligible energy saving for cooling in constructions (Akbari and Konopacki, 2005). In this view, green and cool roofs represent two passive techniques to reduce energy requirement and improve thermal-energy performance in buildings (Santamouris, 2014. Ferrante and Mihalakakou, 2001). In Italy, however, the regulation about the preservation of the architectural and environmental heritage represents a huge restriction to the spread of these technologies, cool roofs in particular, in historic buildings (Pisello et al., 2013).

In this perspective, the purpose of this study is to integrate the strategies above mentioned in a unique and original solution, i.e. an original type of green roof, performing as a *Cool-Green roof*. The feature that characterizes this vegetated roof is the selection, as coating vegetation, of plants that have typical high solar reflectance, high thermal emittance and compact greenery layer, besides further several advantages of green roofs. Additionally, they should have periodical greenery development. Therefore they represent an absorbing surface when it is mostly required, i.e. in winter, and a reflective surface in spring and summer. The proposed *Cool-Green roof*, indeed, has the aim of combining the benefits of both these systems and it is able to dynamically adapt its solar reflectance capability to seasonal environmental variability. In addition, it is characterized by low visual impact, compared to typical high performance cool roofs (e.g. white membranes or coatings, etc.), suitable for application even in historic buildings. These multiple features, and the seasonal resilient behavior of the *Cool-Green roof*, represent the main original contribution of this roof typology with respect to classic cool roof techniques.

In this work, the optical-energy performance of the *Cool-Green roof* is examined through a threefold analytical, experimental and numerical approach via calibrated thermal-energy dynamic simulation, to evaluate the "cool" capability of the solution and its thermal effect in both summer and winter conditions. This solution is studied as application to a historic residential building located in the city center of Perugia, in central Italy, where an attic was constructed over the original Middle Age building structure. In fact, the aerial analysis of the historic building roofs within the ancient city walls showed how the proposed roof system could be suitable for application over many horizontal roofs in the historic urban area. The analysis has been carried out on the basis of the orthophotomap scale 1:5.000 for the city of Perugia (2000) of the Italian Geographical Military Institute. Some examples of such roofs in the city center of Perugia are reported in Figure 1. Moreover, the part of the city within the medieval walls is submitted to declaration of significant public interest by the Italian Ministry of Research, the Italian Government (1961) and the Regional Government (2012), which means that its original appearance must be protected and preserved through non-invasive periodical retrofit interventions and any further changes should comply with local and national architectural preservation authorities. In this view, only clay tiles and greenery-based systems are suitable for application in historic environment, typical of ancient urban centers in Europe and all around the world.

Furthermore, this strategy may provide further benefits where mostly required, since dense historic city centers present the highest Urban Heat Island effect to counteract, together with the lack of green areas and permeable surfaces, because of intense urbanization (Kolokotsa et al., 2013).

In this panorama, the present work builds upon the main research updated background presented below (section 2) with a new strategy for optimizing the thermal-energy performance of new, existing and historic buildings located in dense urban context, by coupling the potentialities of both cool and green roofs.

Fig. 1. Examples of horizontal roofs in the historical city center and case study roof in central Italy (*).

2. RESEARCH BACKGROUND

2.1. Cool roofs and green roofs

Cool roofs are passive cooling systems studied since decades (Berdahl and Bretz, 1997), which surface exposed to the solar radiation is characterized by high solar reflectance and high thermal emittance (Revel et al., 2014). These properties lead to stay cooler than conventional roofing materials under the sun, resulting in lower heat gain entering the building (Akbari et al., 1997). Therefore, cool roofs may introduce three environmental-positive effects: (i) the direct contribution of energy saving for reducing cooling requirements in buildings, (ii) the indirect contribution for mitigating the Urban Heat Island phenomenon (Kolokotsa et al., 2013 and Santamouris et al., 2011) and (iii) the further indirect contribution to the global warming mitigation for reflecting the incoming radiation to the space (Takebayashi and Moriyama, 2012). For their immediate and long-term benefits, relative simplicity and low-cost characteristics, cool roofs have been already investigated through several numerical and experimental researches (Kolokotsa et al., 2012. Levinson et al., 2014), as reviewed in (Santamouris, 2014). In particular, continuous monitoring during summer showed a reduction of heat flux through the building envelope up to 50% of peak value in the case of cool materials (Revel et al., 2014).

Consistently with cool roofs' high potential to save energy for cooling, they were widely used in new constructions and important roof renovations and also their weathering characteristics where analyzed (Paolini et al., 2014). A few contributions analyzing also cool roof winter penalties showed that they are significantly lower than summer benefits even in cold climate, also for the presence of snow covering annulling roof overcooling produced by highly reflective materials (Hosseini and Akbari, 2014. Pisello et al. 2014b). Their application in old historic buildings, instead, is limited due to the regulation for preserving architectural and environmental heritage. In order to minimize the visual impact of these applications, various researchers aimed at elaborating apparently traditional envelope materials with high reflectance capability for improving energy efficiency of historic buildings located in city centers (Libbra et al., 2011; Pisello et al., 2013).

Green roofs, also named "eco-roofs" or "roof gardens", are those roof systems adopting vegetation and growing medium as the outermost layer (Niachou et al., 2001). They can be classified into extensive and intensive technologies, with varying weight and depth of substrate, height of plants, overall performance and, in particular, construction and maintenance costs (Kolokotsa et al., 2013). A key parameter defining thermal insulation properties in green roofs is leaf area index (LAI), i.e. the plan-form area coverage of the leaves, fractional coverage that measures the fraction of the roof surface directly covered by at least one leaf (Kolokotsa et al., 2013). Therefore the higher is the LAI the denser is the vegetation in the green roof and the higher is the reduction of sensible heat load released by the roof (Kolokotsa et al., 2013).

Important energy saving in buildings and environmental benefits may result in the use of green roofs, although depending on their design, local climate conditions and building characteristics (Kolokotsa et al., 2013). Given their potential, different types of green roofs have been used in various countries with confirmed benefits with varying climate conditions and building characteristics, as reviewed in (Berardi et al., 2014). In recent years also multiple researches have been carried out to identify and improve their effectiveness. Considering energy conservation potential of green roofs, Pandey et al. (2013) showed that roof gardens with shrubs are effective in lowering the energy demand for space conditioning in buildings. In that study, two test structures, one with shrubs green roof and the other one with cement based roof, were built and tested over summer in the climate contest of Ujjain, India. They highlighted that foliage height, in combination with the density of the shrub layer, affects the performance of this passive cooling technique, which could achieve about 74% in terms of peak load reduction, compared to cement roof.

Given the ability of green roofs to keep roof surface cooler than traditional materials, reducing building cooling demand, they can be considered a type of cool roof (Ascione et al., 2013), even if characterized by lower solar reflectance than typical cool roofs. Various studies have compared green and cool roofs' thermal-energy and mitigation performance. Zinzi et Agnoli (2012) highlighted the combined winter and summer benefits produced by green roofs, even if their performance is much affected by water content. Regarding their potential in mitigating Urban Heat Island effect, Kolokotsa et al. (2013) studied the effect of cool and green roofs for an office building model under free floating conditions, by performing a comparative analysis

through dynamic simulation under diverse European climates and with varying roofs' thermal properties. They found that cool roofs, i.e. roofs with albedo higher than 0.8, present a negative value of maximum daily sensible heat released in all considered climate conditions. Whereas, for green roofs with high LAI value, the energy released is negative just in the warmest climate. Specific attention was paid to the analysis of green roof microclimate mitigation potential in dense urban configurations, also representative of the historic context taken into account in this work (Taleghani et al., 2014). Most of these works considered extensive roofs planted with grass, without paying much attention to the green roof capability to reflect the short-wave solar radiation, by increasing the urban canopy albedo. Additionally, Santamouris in (Santamouris, 2014) showed that the mitigation effect of a green roof located over a tall building (higher than 10 m) is basically negligible, while some effect is achieved in dense and low rising built areas. In this view, the application of the analyzed *Cool-Green Roof* is properly suitable for very dense urban areas where effective highly performing cool roofs are not applicable and where the average buildings' height is relatively low (around 6-9 meters, i.e.2-3 floors). Additionally, despite the key role of plants' characteristics and maintenance level in determining green roofs benefits, the analysis of leaves reflectance and its impact on thermal-energy behavior of buildings still lacks in this literature field. Therefore, such analysis is the main object of this work, and a promising application of highly reflective green roofs is proposed as new solution for energy efficiency suitable also in historic buildings and as countermeasure again urban heat island in ancient cities.

2.2. Energy efficiency in historic buildings

In Europe, the regulation about the preservation of the architectural and landscape heritage is aimed at balancing building protection requirements with the need for optimized energy efficiency (3encult, 2013). Therefore, in Italy, several innovative effective technologies for energy saving, such as cool roofs, in historic city centers in particular are unlikely applicable (Presidente della Repubblica, Repubblica Italiana, 2004. Pisello et al., 2013). Nevertheless, historic buildings in city centers were recently modified and further upper floors were frequently constructed, and traditional roof coverings were not always replaced by taking into account neither architectural preservation constraints, nor energy efficiency requirement.

In order to overcome these issues, innovative guidelines and effective solutions specifically focused on possible application in historic urban context have been studied during last years (Salata et al, 2014a-b). Ascione et al. (2011) suggested an approach for the energy refurbishment of a historic building located in Southern Italy, by mean of dynamic energy simulation procedures. They demonstrated a potential reduction of the primary energy demand by around 22% for cumulating different retrofit actions. Several studies aimed at developing new materials and passive techniques with low visual impact to be suitable for application in historic contexts. In particular, Kolokotsa et al. (2012) studied the performance of mineral-based coatings as a passive cooling technique that can improve buildings' envelope thermal performance and energy efficiency. Libbra et al. (2011), instead, tested cool tile coverings with the typical red terracotta color for traditional Italian buildings.

3. MATERIALS AND METHODS

3.1. Research procedure

The present study was motivated by considering the necessity to propose innovative, effective and low visual impact solutions for energy saving in new, existing and historical buildings. With a focus on historic buildings, after a multidisciplinary analysis of heritage preservation and architectural policy constraints, the *Cool-Green roof* solution is presented and assessed through experimental and numerical studies. A first botanical survey focused on roof greenery was carried out and the case study was selected to implement the experiment and the field indoor monitoring. The choice of the case study building was carried out by considering building typicality and the possibility to implement a field experimental campaign in order to validate the finding of the numerical assessment about the proposed solution.

The main steps of the research consisted of:

i. analytical study of the *Cool-Green roof* thermal behavior and definition of the research objectives, i.e. the optimization of the short-wave reflectance of the greenery;
ii. preliminary greenery study and selection;
iii. in-lab characterization of its main optical properties;
iv. choice of the case study;
v. indoor continuous monitoring campaign of the building;
vi. development of the numerical dynamic simulation model;
vii. calibration and validation of the model through experimental, in-field and in-lab, measurements;
viii. analysis of the main results in order to compare the thermal-energy performance of the proposed solution, i.e. the *Cool-Green roof*, with respect to the traditional low-performance roof solutions.

In particular, the study of the selected plant consisted of in-lab characterization in terms of solar reflectance and thermal emittance compared to existing roof materials. Therefore, the year-round assessment of the thermal effect of *Cool-Green roof* with respect to existing roof materials is carried out, when applied to the case study historic building. The chosen building is a historic residential construction located in the ancient city center of Perugia, a Middle Age city located in central Italy. As previously mentioned, this building could be considered as representative of Italian historic residential buildings since, as many other buildings in the historical urban Italian context, it is characterized by the recent construction of a new top floor with a concrete slab as the attic roof and roof terrace, with very poor thermal performance (no thermal insulation and low thermal inertia structure). Additionally, it presents a mixed stone/brick and plaster opaque envelope with no insulation panel, such as the large majority of historic buildings in Italy, where traditional retrofits are not allowed to be implemented, according to local regulations on heritage preservation.

After the dedicated analysis of the thermal balance of green roofs in terms of heat and mass transfer, a specific dynamic simulation procedure was chosen in order to perform the thermal-energy modeling of the case study building to be calibrated and validated with monitored data. To this aim, the FASST (Fast All Season Soil Strength) model by Ouldboukhitine et al. (2011) was selected, and EnergyPlus (U.S. Department of Energy, 2014a) dynamic simulation environment was also preferred as reliable tool implementing such model in its calculation procedure.

In the case of the case study building, such as many existing buildings with low possibility to access technical design documents, e.g. historic architectures, the dynamic simulation requires a careful preliminary calibration of the model based on monitored data. In fact, the large number of required parameters affects the reliability of simulations and important discrepancies between predicted and real data may occur. Therefore, the model was calibrated by means of monitored data of indoor temperature in the case study thermal zones, given the lack of consumption due to low-to-zero occupancy level. Moreover, real continuously monitored weather data of the period were taken into account in order to develop a more realistic prediction of the thermal-energy behavior. Additionally, the thermal transmittance parameter of the three opaque wall typologies was field measured for minimizing further uncertainties sources. Calibration is achieved according to (ASHRAE, 2005) through an iterative process of comparison between predicted and measured temperature data by means of two validation indexes, MBE (Mean Bias Error) and RMSE (Root Mean Square Error). In order to obtain an adequate calibration for the case study model, the tolerance error corresponded to ±0.5 and to 1 °C for MBE and RMSE, respectively, according to (ASHRAE, 2005).

Both summer and winter behavior was assessed in terms of primary energy requirement and indoor thermal comfort. Three indoor thermal comfort models were then considered to evaluate indoor environment conditions: (i) Fanger's model, (ii) Adaptive Thermal Comfort (ATC) models and (iii) Thermal Deviation Index model. All three models were considered in the study in order to develop a more exhaustive analysis by taking into account different boundary conditions included within these three reference methods. In fact, the first model, although mainly dedicated to steady-state thermal environment, is the most exhaustive one in terms of analyzed environmental parameters. The second model takes into account the effect of climate variability and human adaptive potentiality. The third one is specifically designed in order to evaluate results

of continuous monitoring campaign and dynamic simulation procedure as used in this work. The first two models are defined in the European reference standard for the assessment of the global energy performance of buildings EN 15251 (2007) and EN ISO 7730 (2005), while the last one is a method proposed in (Pisello et al., 2012). It aims at evaluating building thermal performance starting from dynamic simulation of buildings in free-running conditions. In fact, the TDI (Thermal Deviation Index) is a non-dimensional objective function useful to define the thermal performance of buildings by quantifying the distance from the indoor thermal target condition, as analytically described in (Pisello et al., 2012), where also a good correlation with Degree Hours method is assessed. Therefore, the year-round performance of the proposed *Cool-Green roof* is compared to the current configuration (concrete slab) and to other flat roof covering materials typically used in residential buildings.

3.2. Plant selection

The preliminary step of the research was the analysis of possible plant species to be implemented as *Cool-Green roof*. The most commonly used plant for extensive green roofs are succulents, in particular the Sedum species, i.e. really resistant plants which require low maintenance effort thanks to their characteristics of drought resistance and low growing rate. Also the grass is widely used even if it requests more maintenance effort. However, it provides better coverage and uniformity together with aromatic plants with relatively limited maintenance. Generally, the required characteristics of the plant to optimize the green roof performance are cold and drought resistance, low maintenance during life cycle and full sun exposure attitude (Berardi et al., 2014).

As already mentioned, this specific research aims to analyze the possibility to optimize the short-wave reflectance capability of green roofs in summer, then combining the main features of green roofs and cool roofs when mostly required. Therefore, the plant species to be used should preferably have also the following requirements:

- white or light pigmentation of leaves or flowers, in order to have high solar reflectance in summer, allowing natural cooling of the building and its surrounding;
- seasonal deciduous leaves in winter period, so that the soil allows heat absorption in the cold season.

Consistently with previous considerations, *Helichrysum Italicum* “Curry plant” has been selected (Fig. 2). The choice was also let by operative reasons of availability and maintenance of the plant. Moreover, the selected species widely corresponds to the established target, as it is an aromatic herbaceous perennial evergreen bushy plant, typical of Mediterranean Climate countries, with very light color foliage and flowers, already used to cover ground areas, walls and pergolas. It must grow up in full sunny exposure, such as typical unshaded roof surfaces, and it does not need much care and any irrigation in temperate climate areas, just a well-drained soil (Voltolina, 2001). The only characteristic to be evergreen was disregarded, but it may be replaced by pruning the greenery once a year, at the beginning of the winter season, when the growing velocity is relatively limited, as also requested for the correct maintenance of the selected greenery.

Fig. 2. *Helichrysum Italicum* (“Curry plant”) used in this study: (a) foliage, (b) paving installation, (c) plant used for the sample development.

4. THERMAL-PHYSICS OF THE *COOL-GREEN ROOF*

In order to analyze the thermal-physics behavior of the proposed solution, all the physical phenomena interacting with its performance were investigated and the reference analytical approach followed in this analysis are reported as follows. Therefore, the analytical clarification of the *Cool-Green roof* effect is here addressed. To this aim, the role of high albedo greenery and its optimization with varying weather and climate conditions was studied. The main heat fluxes through the traditional green roofs were identified by

taking into account the recent research development in this field (Ouldboukhitine et al., 2011) and, in particular, those analytical formulations operating in the dynamic simulation environment (Sailor et al., 2008). The graph in Figure 3 reports these fluxes participating to the roof energy balance, where particular attention was paid to those terms affected by the selection of the cool greenery, i.e. the foliage albedo α_f

---

Fig. 3. Different fluxes participating to the green roof energy balance.

Given the focus of the work, specific analysis was carried out while considering those terms mainly affected by the canopy albedo. Therefore, the evaporative and conductive heat fluxes through the roof soil and, then, to building envelope were only briefly dealt with, even acknowledging their role in affecting humidity and air-conditioning need (Ouldboukhitine et al., 2011).

The mathematical formulation of the problem was proposed by Ouldboukhitine et al. (2011) which considered the energy balances of the green canopy and the soil layers. Since the focus here is the role of the canopy albedo, double analysis of such property has been carried out by combining the role of the (i) greenery, properly selected as described in section 3.1, and the (ii) soil, as possible alternative to the cool plant in winter conditions. Therefore, following the proposed approach, both these finishing were considered as canopy layers, since they are exposed to the solar radiation in different periods during the course of the year. Afterwards, both the thermal balances at leaf surface and at soil surface were investigated, as described in sections 4.1 and 4.2, respectively.

4.1. Energy balance at foliage layer

Equation (1) describes the energy balance at foliage layer ("f" subscript), by considering the thermal fluxes previously mentioned in the analysis of the green roof behavior.

$$F_f(t) = \sigma_f\left[I_f^s(t)\cdot\left(1-\alpha_f\right) + \varepsilon_f I_f^l(t) - \varepsilon_f \sigma T_f^4(t)\right] + \frac{\sigma_f \varepsilon_f \varepsilon_s \sigma}{\varepsilon_f+\varepsilon_s-\varepsilon_f\varepsilon_s}\left(T_s^4(t) - T_f^4(t)\right) + H_f(t) + L_f(t) \quad (1)$$

The explanation of all the letters and symbols is reported in the nomenclature section, but here the focus is dedicated to the role of the foliage albedo α_f, particularly important where the solar radiation contribution $I_f^s(t)$ reaching the *Cool-Green roof* is high.

The sensible heat flux at the *Helichrysum Italicum* layer is affected by the temperature difference between the foliage surface and the air $T_{a-f}(t)$, by the wind speed $W_{a-f}(t)$ affecting the convection thermal transfer, and the LAI, i.e. the Leaf Area Index. This index describes the non-dimensional ratio between the projected greenery area on the soil and the soil unit area. In particular the definition of H_f was carried out by Deardoff (1987), as reported in (2). It does not depend on the foliage albedo but it is affected by the surface temperature of the foliage, indirectly influenced by the foliage albedo, as investigated in this work.

$$H_f(t) = \left(e_o + 1.1\cdot LAI\cdot \rho_{a-f}\cdot C_{p-a}\cdot C_f\cdot W_{a-f}(t)\right)\cdot\left(T_{a-f}(t) - T_f(t)\right) \quad (2)$$

The constant value 1.1 determined by Deardoff (1987) takes into account the heat transfer from the stems, twigs and limbs, while the green roof calculation model implemented in EnergyPlus platform considers the windless exchange coefficient e_0 equal to zero.

Focusing on the net radiation (NR) flux through a leaf, indirectly determining the canopy thermal characteristics, a key model simplification should be noted. In fact, the FASST model assumes the canopy to behave as a dense foliage layer exposed to the solar radiation, i.e. "big leaf hypothesis", covering the roof by

the σ_f portion. In order to make this assumption as much reliable as possible, the choice of the greenery was governed by its geometry: very high density and relatively flat homogeneous surfaces determined by numerous and small leafs reflecting solar radiation by σ_f (foliage density) and according to its albedo α_f .

Also the variation of superficial properties of transmittance, reflectance and emittance with varying wavelength λ is considered in the problem. Therefore, the net radiation NR exiting the "cool leaf" is reported as follows (3):

$$NR_f(t) = \int_0^\infty \left[\left(1 - \tau_f(\lambda) - \rho_f(\lambda)\right) \cdot I_f(\lambda, t) - \varepsilon_f(\lambda) B(\lambda)\right] \mathrm{d}\lambda \quad (3)$$

where $\tau(\lambda)$, $\rho(\lambda)$ and $\varepsilon(\lambda)$ represent the spectral transmittance, reflectance and emittance of the leaf (foliage), respectively. $I_f(\lambda, t)$ is the solar spectral irradiance at the leaf surface. $B(\lambda)$ is the Plank function.

Since 95% of the total energy reaching the Earth surface is included in the range of the short wave [300nm;2500nm] (Libbra et al., 2011), and since typical objects at environmental temperatures emit in the range of long waves [2800 nm;40000nm], equation (3) could be rewritten by separating these two ranges: one for the short waves "s" and the second one for the long waves "l" (4).

$$NR_f(t) \cong \left(1 - \tau_f^s - \rho_f^s\right) \cdot I_f^s(t) + \left(1 - \tau_f^l - \rho_f^l\right) \cdot I_f^l(t) - \varepsilon_f^l \int_{\lambda_0}^{\lambda_1} B(\lambda) \mathrm{d}\lambda \quad (4)$$

where λ_0 and λ_1 correspond to 2800 nm and 40000 nm, respectively. Since for most of the leaf typologies transmittance and reflectance in the long wave range are negligible, while the thermal emittance is almost equal to the unity without important loss of accuracy at this level of approximation, the net radiation at foliage level could be written as the first part of the energy balance in equation (1) as follows (5):

$$NR_f(t) \cong \left(1 - \tau_f^s - \rho_f^s\right) \cdot I_f^s(t) + I_f^l(t) - \sigma T_f^4(t) \quad (5)$$

The optimization of the passive cooling contribution of the presented solution mainly consists of the decrease of the first addend of equation (5) through increasing foliage albedo. Since the chosen plant layer is assumed to be very dense consistently with the hypotheses of FASST model, τ_f^s is meant to be zero, as already assumed in (1).

4.2. Energy balance at soil layer

The surface characterization of the soil and the greenery on top mainly determines the thermal properties of the same soil layer and the thermal exchange through the roof. The soil energy balance (Ouldboukhitine et al., 2011) used by the selected simulation tool is consistent with the one reported in equation (1) by considering the soil properties instead of the foliage ones. Also in this case, the sensible heat flux is influenced by the wind speed in the air-foliage interface and the temperature difference between the soil surface and the surrounding air. Therefore, this last aspect mainly influences the thermal performance of the roof, and the soil relatively higher thermal absorption capability could be taken into account for optimizing the green roof performance even in winter conditions. In particular, the sensible heat exchange is reported in equation (6) given by (Ouldboukhitine et al., 2011).

$$H_S(t) = \left(e_o + \rho_{a-s} \cdot C_{p-a} \cdot C_h^s \cdot W_{a-f}(t)\right) \cdot \left(T_{a-f}(t) - T_S(t)\right) \quad (6)$$

Also in this case, for the latent heat flux analysis, the reader is referenced to (Ouldboukhitine et al., 2011).

4.3. Thermal analysis of the *Cool-Green roof*

The two unknown T_f and T_s are the surface temperature of the foliage and of the soil, mainly affecting the thermal behavior of the green roof and characterizing the peculiar behavior of a *Cool-Green Roof* with respect to a generic green solution. Additionally, by optimizing the greenery choice in the "cooling" direction in summer, the foliage surface temperature T_f represents an important indicator of the *Cool-Green Roof* performance. In order to solve the foliage and the soil energy balances, the fourth order temperature terms were linearized in the numerical calculations by Deardoff (1987). Therefore, the time integration of the system through an explicit first order algorithm is carried out for the purpose of this work (7-8):

$$T_f^4(t+\Delta t) \cong T_f^4(t) + 4 \cdot T_f^3(t)\big(T_f(t+\Delta t\big) - T_f(t) \tag{7}$$

$$T_S^4(t+\Delta t) \cong T_S^4(t) + 4 \cdot T_S^3(t)(T_S(t+\Delta t) - T_S(t) \tag{8}$$

After the linearization process, the role of the two temperatures, i.e. greenery and soil surface, could be investigated in its threefold thermal-physics effect on: (i) the performance of the building covered by the green roof, (ii) the surrounding microclimate, (iii) the urban mesoclimate and heat island phenomena (Santamouris et al., 2011).

5. EXPERIMENTAL ANALYSIS

5.1. In-lab measurement of the thermal-physics properties

In order to accurately characterize the selected plant and other materials commonly used for flat roof covering, experimental analyses have been carried out by measuring significant optical properties of the selected materials. These properties are useful for understanding their in-field behavior and for the elaboration of a reliable dynamic simulation model of the building. The selected materials are:

i. *Helichrysum Italicum* plant, selected for its cool-green property;
ii. concrete layer, the material currently covering the building roof;
iii. green grass, typically used in walkable green roof terraces;
iv. brown soil, for its possible use as external layer in winter;
v. bitumen membrane, usually applied as flat roof coating.

Homogeneous and smooth samples for each material have been prepared according to international reference standards (ASTM E903-96; ASTM C1371-04a, 2010). The study of samples' properties has been carried out through an experimental measurement campaign of solar reflectance and thermal emittance. All selected materials have been in-lab tested, except for the bituminous membrane that was already analyzed in (Lawrence Berkeley National Laboratory, 2000).

Solar reflectance measurements were carried out by spectrophotometer with integrating sphere Shimadzu SolidSpec 3700 (Shimadzu Corporation, Kyoto, Japan), which characteristics are reported in Table 1 and Figure 4 (a). In particular, the integrating sphere has a diameter of 60 mm and it is internally coated with a layer of barium sulfate (perfectly diffusing white). This instrument is capable of measuring the spectral characteristics of materials over the solar spectral region in the range 300÷2500 nm. The solar hemispherical reflectance of the samples is evaluated by following the test method procedure of the international reference standard (ASTM E903-96), considering the solar spectrum described in (ASTM G173-03, 2012). The solar reflectance measurements were obtained through a two-step procedure: (i) measurement of relative reflectance with respect to the standard white by mean of spectrophotometer and (ii) data post-processing according to the international reference standard (ASTM E903-96). Spectral measurements were performed with a resolution step (i) of 0.5 nm, in the spectral range 300-400 nm, (ii) of 1 nm, in the range 400÷1702 nm, and (iii) of every 5 nm, in the range 1705÷2500 nm, according to (ASTM E903-96). Due to the possible non-homogeneous characteristics of some samples, five different measures have been performed for each specimen, with varying the sample position with respect to the beam spot of

the spectrophotometer. The final solar reflectance of the material is obtained as the average of the measures by considering the reference solar spectrum (ASTM G173-03, 2012).

The portable differential thermopile emissometer used in order to characterize the thermal emittance of the samples is an AE1 RD1 Emissometer D&S with scaling digital voltmeter (Devices & Services Co., Dallas, Texas). Its characteristics are reported in Table 1 and Figure 4 (b). The instrument is composed of a differential thermopile radiant energy detector, a heater, and a heat sink with a flat surface. The measurements were carried out by following the procedure of the international reference standard (ASTM C1371-04a, 2010), after an initial careful calibration of the apparatus. However, due to the non-uniformity of some plants' samples, measured thermal emittance values for "Grass", "*Helichrysum Italicum*" and "Soil" were deduced from acknowledged focused literature in this specific measurement field (French et al., 2000).

5.2. In-field measurement of external walls' thermal transmittance

In order to accurately characterize the thermo-physical properties of the building's external walls, in-field measurements of the thermal transmittance have been carried out in the case study apartment. In particular, three areas of the external walls of the monitored thermal zones were identified after acknowledging different envelope structures by mean of infrared camera and architectural analysis of the different volumes constituting the ancient building. Given the lack of homogeneity in the thermal properties of the opaque envelope systems, typical of historic buildings, large plate Teflon-based heat flowmeter was used, which characteristics are reported in Table 1 (Part C.). The area of the square plate (2500 cm^2) was selected in order to measure the thermal transmittance of all the three selected wall typologies described within the dynamic simulation environment. The large heat flowmeter plate is indeed able to detect stones, brick and plaster portions of each irregular wall in the same measurement. The data analysis was carried out according to the international reference standard for thermal transmittance field measurement and relative post-process method (ISO 9869, 1994).

Table 1. Technical features of the experimental measurement apparatus (A. spectrophotometer, B. emissometer, C. heat flowmeter plate).

Fig. 4. (a) Spectrophotometer, (b) emissometer and (c) heat flowmeter apparatus instruments for in-lab and in-field experimental analysis.

6. CASE STUDY

6.1. The building

The thermal-energy performance analysis of the proposed *Cool-Green roof* is carried out when applied to a historic residential building located within the medieval walls in the city center of Perugia, in central Italy. The building, originally built in the XVI century, consists of 4 floors: the common atrium is located at ground floor and one residential unit per floor is located in the upper floors, as reported in Figure 5(a). Furthermore, the building has a small internal courtyard, providing daylight to the rooms and accommodation for pipes and the external units of HVAC systems located in the apartments. The study focuses on the apartment located on the top floor of the building described in Figure 5 (b) and Table 2, since the purpose of the work is to evaluate the effect of varying thermal-physics characteristics of the roof on the monitored indoor environment.

The building presents traditional materials such as a masonry resistant structure, consisting of brick, stone and travertine, covered by cement and gypsum plaster on the inner side, without any insulation panel.

As previously described in section 5.2, continuous in-field measurements have been carried out in order to characterize the thermal transmittance of the external walls. Measured values are reported in Table 2. Similarly, the roof is made of wood resistant structures and bricks. The only anomaly detected in the envelope consists of the recent (around 1960) construction of a new attic volume over the ancient roof. For what concerns fixtures, there are wooden doors and window frames, double glazing panels and external wooden movable shutters. The entrance has North-East orientation and the building is surrounded by narrow alleys on three sides. Additionally, part of the North-West side of the structure is enclosed to another residential building, and the South-East area is adjacent to a taller commercial building. The main windows are North-East (two rooms with two windows each) and South-West (one room with one window) oriented. Other smaller openings are in other facades and the internal courtyard. The apartment is served by a methane boiler for space heating and heat water production while, at the moment, there is no cooling system. Although designed for residential purpose, the thermal zones were only rarely used as meeting rooms by 2-3 people, with a frequency of about 3 hours per week. Buildings surrounding the case study have similar height, exterior envelope materials and architectural configuration, as showed in Figure 1. Since the study is focused on free-floating conditions, no further details are given about the HVAC systems, given that it was not operative during the course of the monitoring period. All these characteristics affecting surrounding microclimate and the detailed geometry of surrounding buildings were described within the dynamic simulation environment.

Table 2. Technical data of the case study building.

Fig. 5. (a) Building façade, (b) living room and (c) top floor plan.

6.2. Monitoring campaign

In order to develop more realistic simulations of the thermal-energy behavior of the case study building, the building model was calibrated by means of measured values of indoor temperature in the case study thermal zones. Moreover, real continuously monitored weather data of the period, taken from a dedicated complete weather station located on the roof of a university building in close proximity, were considered to develop a more realistic predictive model. Technical characteristics of the monitoring station are described in a previous work by the same authors (Pisello et al., 2014a).

The campaign of indoor temperature measurements was carried out by equipping the apartment with two temperature data-loggers EBI 20-T (Ebro Electronic, Ingolstadt, Germany) with internal sensor to measure and automatically record air temperature data every 10 minutes. Data-loggers have a temperature measuring range between -30°C and +60°C, with a sampling rate from 1min to 24h. The instrument has an accuracy of ±0,5°C for temperature from -20°C to +40°C and ±0,8°C for the boundary range. Data-loggers were located in two rooms facing different orientations, as specified in Figure 5. The first one was placed within the entrance room (ER) of the apartment, which is positioned in the Northern corner of the building with two North-East oriented windows and one North-West facing window, as indicated in Figure 5(c). The second one was placed within an innermost study room (SR) just facing a small internal courtyard. Measurements were performed in the free-running apartment for a period of two months, from April 21st to June 18th 2013. In this way, a wide variety of weather conditions was monitored for an exhaustive calibration procedure, from initial cold climate (late winter conditions) to almost summer temperatures in the last days of measurement. Data-loggers were programmed to perform measurements every 10 minutes, which were finally used for the calibration. During the monitoring period, the building was not occupied except for some hours per month for meeting purpose by 2-3 people. Additionally, HVAC systems were not operating. Therefore both these observations were taken into account during the calibration procedure. The same temperature data-loggers were combined with the heat flowmeter apparatus (with its dedicated data-logger)

in order to perform the field measurement of the three opaque wall typologies. In fact, given the intrinsic uncertainties characterizing thermal-physic properties of historic buildings, dedicated measurements were performed in winter period December 2013-January 2014 according to (ISO 9869, 1994). Therefore the thermal transmittance values were calculated and included into the dynamic simulation model of the case study building.

6.3. The energy model

In order to assess *Cool-Green roof* performance on the case study building, the dynamic simulation model of the residential building was carried out within EnergyPlus (U.S. Department of Energy, 2014a) simulation environment with varying roof layout and experimentally measured properties. Firstly, the architectural configuration of the structure was implemented by describing geometry, internal thermal zones, thermo-physical characteristics of the building envelope and its technical elements and materials. Also the distribution of the surrounding buildings was considered to take into account possible inter-building effects. Concerning green roof implementation, green roofs can be modeled in EnergyPlus as the outermost layer of a rooftop construction by means of the Fast All Season Soil Strength (FASST) vegetation model (Ouldboukhitine et al., 2011), as described in section 4. This model accounts for (i) long and short wave radiative exchange within the plant canopy, (ii) plant canopy effects on convective heat transfer, (iii) evapotranspiration from the soil and plants, (iv) heat conduction, (v) storage in the soil layer and (vi) track of moisture-dependent thermal flux (Ouldboukhitine et al., 2011). The green roof, then, can receive water during the simulation from an irrigation system and/or from site precipitation. This last option was selected, as the proposed greenery does not require any irrigation system. After the definition of green roof initial properties (i.e. growing media depth, average plants height, thermal properties, as leaf reflectance and emittance, plant canopy density and leaf area index LAI, minimum stomatal conductance and soil moisture conditions), the model provides a quantitative and physically-based building energy simulation tool computing the effects of green roof in terms of superficial temperature of the foliage and of the soil, affecting the thermal-physics behavior of the apartment, which is analyzed in this work.

The performance analysis of the proposed green roof application concerns the apartment on the top floor of the building, which is a non-occupied free-floating thermal area.

6.4. Climatological data

The thermal-energy simulation was carried out in both summer and winter conditions, by taking into account climate boundaries of Perugia, Italy. The city, located in central Italy, is characterized by 2289 degree days. Table 3 reports the principal monthly climate data of the location for outdoor dry-bulb temperature and solar radiation. The considered values derive from the weather station encoded as Perugia 161810 of the IGDG (Italian Climatic data collection “Gianni De Giorgio”), positioned at 213 m above the see level. The weather hourly data of the s

ite are collected from the database of the Europe WMO Region 6 (U.S. Department of Energy, 2014b) used by EnergyPlus calculation engine. The thermal-energy year-round numerical analysis was carried out by comparing the performance of the apartment with *Cool-Green roof* with respect to the same thermal zone with the current roof configuration and other roof coverings.

Table 3. Principal monthly characteristics of the weather conditions of the considered site.

6.5. Roof scenarios

In order to perform a comparative analysis on the effect of *Cool-Green roof* on the case study building with respect to other flat roof coverings, nine different models of the building have been developed starting from the actual calibrated model, with varying the roof coating and insulation characteristics. The nine roof

configurations considered in this analysis include the actual configuration and various retrofit solutions, including the finishing materials tested through the in-lab procedures and previously described in section 5.1, as follows:

1. Concrete Roof (CR): the coating material is concrete, the current outermost layer of the building roof, such as in other historic buildings subject to non-authorized building volume extension;
2. Bitumen Roof (BR): the coating material is a black bitumen membrane, often used in flat roofs configuration;
3. Insulated Bitumen Roof (I-BR): the coating material is the black bitumen membrane, and a 6 cm strawboard-like glass-fibre layer is added as insulation;
4. Green Roof (GR): the coating material is a traditional extensive green roof package with green grass as vegetation outermost layer;
5. Insulated Green Roof (I-GR): the coating material is the traditional extensive green roof package with green grass, and a 6 cm strawboard-like glass-fibre layer is added as insulation;
6. *Cool-Green Roof* (CGR): the coating material is an extensive green roof package with *Helichrysum Italicum* plant as vegetation outermost layer;
7. Insulated *Cool-Green Roof* (I-CGR): the coating material is the extensive green roof package with *Helichrysum Italicum* plant, and a 6 cm strawboard-like glass-fibre layer is added as insulation;
8. Soil-Green Roof (SGR): the coating material is a green roof package with only soil, without any grown plant on the top;
9. Insulated Soil-Green Roof (I-SGR): the coating material is the green roof package with only soil, and a 6 cm strawboard-like glass-fibre layer is added as insulation.

Table 4. Green roof properties.

The nine roof scenarios were characterized by considering the radiant properties of roof coatings experimentally examined (Section 5.1) and already tested by internationally acknowledged labs (bitumen membrane, Lawrence Berkeley National Laboratory, 2000). Regarding the three green roofs, also other significant properties were defined, such as growing media depth, average plants height and LAI (Table 4). Values of LAI were set for each green roof by taking into account indications of Scurlock et al. (2001), reporting the statistical distribution of global leaf area index data by biome from field measurements. Furthermore, average annual precipitation rate was specified according to data from Aeronautica Militare Italiana (2014) relative to the city of Perugia and the natural irrigation amount was set just in the green roof analytical model.

7. DISCUSSION OF RESULTS

7.1. Experimental tests

The measured spectra of the tested samples are shown in Figure 6(a) with respect to the solar spectrum, and the concise calculated values of solar reflectance, with the standard deviation error, are reported in Table 5. Data of the bituminous membrane have been are reported in the same table for comparison purpose. By comparing the reflectance spectra, it is evident that the greenery, i.e. “Grass” and “*Helichrysum Italicum*”, has notable performance in the range 700÷1300 nm, with respect to the “Concrete”. In particular, the “*Helichrysum Italicum*” has also a better solar reflectance in the last part of NIR, even if slightly lower than concrete. Its light color produces a notable increase of solar reflectance also in the visible zone of the solar radiation spectrum, up to 700 nm. In fact, R_{uv} and R_{vis} values of the “*Helichrysum Italicum*” sample are higher by 10% and 16%, respectively, in comparison to the classic “Grass” sample. Ultimately, the “*Helichrysum Italicum*” sample exhibits quite good R_{solar}, equal to 44%, if compared to other materials. The “Soil” sample, instead, has the lower value of reflectance in the whole spectrum. Anyway, all the tested samples have a solar reflectance higher than the reference bitumen membrane (Lawrence Berkeley National Laboratory, 2000).

Thermal emittance was measured by portable emissometer and the results were compared to the existing literature in this field (French et al., 2000). Given the operative instrument limitations for emissivity measurements in plants' samples according to the international reference standard (ASTM C1371-04a, 2010), measured thermal emittance values for "Grass", "*Helichrysum Italicum*" and "Soil" were deduced from previously published studies highly focused on this kind of measurements, as reported in Table 5.

The thermal transmittance of the three opaque wall typologies was measured as specified in sections 5.2 and 6.2 during the winter period December 2013-January 2014. Figure 6(b) reports the measured thermal transmittance converging to asymptotical values of the three walls according to the procedure specified in (EN ISO 6946, 2007) for heavy elements, i.e. with specific heat per unit area of more than 20 kJ/(m^2K). Typology 1 refers to the highest thickness stone façade. Typology 2 refers to a North facing wall recently renovated with thin brick layers without any insulation, typology 3 refers to wall sections under windows. The thermal-physic properties of all these systems were included into the dynamic simulation model of the case study building.

Fig. 6. (a) Solar reflectance of the various samples and the solar spectrum; (b) thermal transmittance of opaque wall typologies.

Table 5. Solar Reflectance and Thermal Emittance properties of the different materials.

7.2. Calibration procedure

As above mentioned, the building energy model was calibrated on monitored indoor temperature data, in order to obtain more realistic energy-behavior prediction. After the simulation of the initial building model, the discrepancy between simulated and real indoor temperatures was quantified by means of MBE and RMSE indexes for both the control thermal zones, i.e. the entrance room (ER) and the study room (SR), getting the values reported in Table 6. Calculated indexes were far from the validation criteria previously specified in section 3.2. From an accurate comparison of temperatures, simulated temperatures were generally lower than the measured ones, and the discrepancy was higher in the initial monitoring period, when the outdoor weather was still quite cold for the typical weather conditions of the period. This discrepancy decreased in the final period of measurement, when the warm season started.

Fig. 7. Measured and simulated indoor temperatures for ER and SR.

Table 6. MBE and RMSE values before and after the calibration process.

Accordingly, the model was calibrated through a process of iterative modifications, to take into account the collaborating thermal capacity of the case study apartment and the adjacent buildings. The included modifications consisted of: (i) removal of windows' shielding system, (ii) increase of opaque envelope thickness, and (iii) increase of internal gains. Moreover, a more accurate climate file was implemented using real monitored weather data of year 2013 in the case study area. Finally, the model was considered as calibrated and the calibration indexes are reported in Table 6. Both MBE and RMSE indexes determined for the two rooms were considered as valid for the purpose of this work, as they were found to be widely included in the tolerance range, according to (ASHRAE, 2005). The comparative analysis of measured and simulated indoor temperature for both initial and calibrated model for the entrance room ER and the study room SR (Fig. 7) confirms the applicability of the building model. Temperature profiles have low fluctuation

and the value is nearly constant during the day. This is due to the huge collaborating mass of the building and to the fact that windows have been keeping closed for most of the time since almost none usually occupy the apartment.

7.3. Indoor thermal analysis

For the goal of assessing the effect of *Cool-Green roof* on the case study building compared to other flat roof coatings, the year-round thermal-energy dynamic simulation was carried out in free-floating conditions, with varying roof scenarios. Then, the performance of the nine coatings, listed in section 6.5, is compared in terms of indoor operative temperature (EN 15251, 2007). Figure 8 reports the profile of the attic operative temperature (case study apartment) with respect to the outdoor dry-bulb temperature and to the solar radiation during one central week for each season. The temperature profiles show how green roofs are able to decrease the indoor operative temperature in summer, up to 3°C compared to the current Concrete Roof (CR) and 6°C compared to Bitumen Roof (BR). In fact, the BR causes a temperature increase of about 3°C, due to the highest solar absorption property. In particular, the *Cool-Green roof* (CGR) presents lower temperatures by about 1°C than the standard grass Green Roof (GR). The Soil (SGR) roof, instead, due to its high solar absorption capability, produces higher temperatures than the other greeneries, even if the highest temperature peaks are lower than the BR. The effect of the additional insulation layer, instead, is considerable only for the less effective configurations, i.e. I-BR and I-SGR. It is not perceived with the high reflectance green roofs (I-GR and I-CGR). Furthermore, the comparison of CR and I-BR shows how, in summer, the higher solar reflectance (of CR vs. I-BR) is more effective than the extra thermal insulation (I-BR).

In winter, the three green roofs are able to increase the indoor attic operative temperature, up to 2°C compared to the current CR, and about 3°C compared to BR, due to the high thermal insulation produced by the vegetated layers in general. Moreover, the combination of green roof and insulation of scenarios I-GR, I-CGR and I-SGR produces even further benefits in terms of temperature increase, by about 0.5°C in all the configurations. Accordingly, temperature profiles of the three configurations with green roofs, even more with the further insulation, are able to dampen down the outdoor weather forcing, as showed by the outdoor temperature and the solar radiation profiles. Whereas, the current Concrete Roof and the Bitumen Roof configurations make the attic more sensitive to the outdoor fluctuations.

The year-round results show that the main effect of *Cool-Green Roof* consists of decreasing temperature in summer conditions. This is due to the high foliage height and the density of the shrub layer, which results in a smaller exposed area to the solar radiation, in combination with the higher albedo of the plant foliage. In fact, given the higher solar radiation contribution in summer than in winter months, the benefit of the light coating is highlighted when its effect is mostly required, i.e. in hottest months. These results are confirmed by the capability of the proposed green roof to reduce the number of hours when the indoor operative temperature is higher than 26°C in summer and lower than 20°C in winter, as detailed in Tables 7 and 8 for summer and winter, respectively.

Fig. 8. Attic operative temperature hourly trends for the different scenarios.

Table 7. Number of hours with temperature higher than 26°C in summer.

Table 8. Number of hours with temperature lower than 20°C in winter.

Further analyses were performed in order to describe the compared roof solutions by means of thermal comfort models. This analysis is not aimed at performing environmental comfort integrated assessment, but it is aimed at comparing the indoor thermal free-floating conditions by taking into account acknowledged assessment models for comparative purpose. In particular, in both summer and winter conditions, the results

were compared by means of three comfort models: Fanger's model (EN ISO 7730, 2005), ATC model (EN 15251, 2007) and TDI model (Pisello et al., 2012). These models were implemented in this study in order to evaluate seasonal indoor thermal conditions influenced by roof techniques by considering (i) low resolution indicators, i.e. PMV and PPD, (ii) high resolution models (ATC) taking into account also human capability to adapt personal thermal sensitivity to the variation of external thermal parameters, and (iii) parameters calculated by considering dynamically variable indoor thermal conditions as simulated by means of numerical models, i.e. TDI, as implemented in this study. Figure 9 reports the results for PMV (Predicted Mean Vote) and PPD (Predicted Percentage of Dissatisfied) of Fanger's model. In summer assessment, results about insulated green roofs (I-GR and I-CGR) are not depicted, since they are almost equal to those of green roofs (GR and CGR) and such negligible difference is not visible in the graph. For the same reason, in winter GR, CGR and SGR are represented by mean of a single line. The same was considered for the three insulated green roofs (I-GR, I-CGR and I-SGR). Summer results show how green roofs are able to reduce operative temperature, keeping the PMV index (EN ISO 7730, 2005) within the thermal comfort area for most of the season. In particular, the percentage of overheating hours in the *Cool-Green Roof* scenario is zero (Table 9). On the other hand, it causes an increase of overcooling hours from the value registered for the Green Roof, as summarized in Table 9. However, by considering the percentage of discomfortable hours, both green roofs are more effective than BR, I-BR and CR, as expected. Instead, PPD (EN ISO 7730, 2005) does not highlight notable differences among the different scenarios (except for BR), since it takes into account both overheating and overcooling together, to predict the percentage of thermally dissatisfied people. In particular, both green roofs are capable to keep PPD index under the 10% limit for most of the season (Fig. 9). In winter, as expected from the previous analyses, both PPD and PMV indexes for all four scenarios are out of the comfort zone, since the building is studied in free-floating conditions. However, the situation is slightly improved by adding the insulation. Moreover, both indexes are substantially equal for the three green roofs and the three insulated green roofs, respectively. Findings of the Adaptive model (ATC), reported in Table 9, show fewer differences between the different roof coatings, due to the wider comfort zone. However, the assessment of Degree Hours (EN 15251, 2007) for both summer and winter points out the best performance of green roofs. In particular, the *Cool-Green roof* and the insulated *Cool-Green roof* in summer produce only 12 and 10 Degree Hours, respectively, and the best solution in winter is the I-SGR with 26631 Degree Hours.

TDI results, illustrated in Figure 10, finally confirm the benefits of green roofs compared to the CR and the BR, both in warm and cold season. Specifically in the hottest months, the *Cool-Green roof* configurations optimize the thermal indoor performance, with nearly zero TDI values. Instead, in winter both grass and soil coatings, combined with the insulating layer are able to optimize indoor thermal comfort, due to the further insulation contribution with respect to the poor concrete layer and the simply insulated I-BR. However, all winter indexes are relatively high, meaning that the thermal zone is far from the thermal target in free floating conditions. Finally, the year-round analysis of TDI shows that the most performing solution is the combination of I-CGR in summer and I-SGR in winter, achievable by pruning the greenery at the beginning of the winter season.

Fig. 9. PMV and PPD indexes for the different scenarios.

Table 9. Fanger's and Adaptive Thermal Comfort model results for the different scenarios.

Fig. 10. TDI indexes for the different scenarios.

7.4. Energy analysis

The comparison of primary energy requirement for cooling and heating of the different scenarios is here carried out in summer and winter season, respectively. Then, aggregated primary energy requirements for the

whole year are analyzed. For this purpose, simulations were performed with reference to two seasonal temperature set-points, i.e. 26°C and 20°C, in summer and winter, respectively. Monthly primary energy requirements for heating and cooling are depicted in Figure 11 and yearly aggregated results are reported in Table 10. Energy analysis results are consistent with data from previous free floating analysis. In fact the BR scenario has the highest primary energy need in both summer and winter, followed by the current CR and the I-BR. Primary energy requirement with the *Cool-Green roof* and insulation (I-CGR) is equal to only 13.5 kWh in summer and 17155.7 kWh in winter, compared to 2024.0 kWh and 34012.3 kWh, respectively, with BR, and 489.9 kWh and 29052.7 kWh, respectively, with CR. The percentage decrease of seasonal primary energy requirement in case of combined green roofs and insulation corresponds to up to 97% for cooling and up to 42% for heating. In particular, the non-insulated and insulated *Cool-Green roofs* optimize energy consumption in summer, while the insulated I-GR, I-CGR and I-SGR are the best performing in winter. In fact, all green roofs register negligible differences in winter, in the order of by 1-2%. Finally, the energy analysis show how the combination of vegetated roofs and insulation layer is the best performing in terms of year-round assessment, while the only insulation of non-permeable and low-reflectance roof solution (I-BR) decreases the energy efficiency of the attic in both winter and summer

---

Fig. 11. Primary energy requirement (a) for cooling and (b) for heating.

Table 10. Annual primary energy requirements.

8. CONCLUSIONS AND FUTURE DEVELOPMENTS

This study aims to contribute to the research on the thermal-energy behavior and the potential urban climate mitigation of green and cool roof solutions in urban areas. In fact, a specific type of green roof, named *Cool-Green roof*, has been developed as innovative solution suitable for application in new constructions and existing, even historic, buildings. Therefore, the proposed system was studied as non-impactive energy retrofit in a residential construction in central Italy, chosen as case study. The peculiar feature of this green roof is the use, as vegetation outermost layer, of light-colored plants with high short-wave solar reflectance capability. A dedicated analytical assessment of the *Cool-Green Roof* behavior is dealt with in this study. The goal is achieved by using the *Helichrysum Italicum* plant, a very resistant dryland shrub typical of Mediterranean countries, which can grow in the climate context of central Italy with limited maintenance effort.

Experimental analyses showed that the proposed *Cool-Green roof* is able to reflect the total solar radiation by 44%, i.e. 6% more than a concrete roof, which is the coating currently installed over the monitored case study building, and 7% more than a traditional green grass roof. The thermal-energy dynamic analysis, carried out for the residential building covered by the *Cool-Green roof*, proved that the application of this solution can reduce the number of overheating hours (T_{op}>26°C) in summer by about 98%, and the number of overcooling hours (T_{op}< 20°C) in winter by about 1%, compared to concrete roof. The percentage decrease of discomfort hours can be further decreased in winter if the *Cool-Green roof* is combined to a thin insulating layer. Moreover, the winter penalty produced by highly reflective foliage corresponds to less than 1% if compared to the traditional green grass roof. Further analyses on comfort indexes and primary energy requirement confirmed the effectiveness of the proposed solution in improving indoor thermal comfort conditions and reducing attic energy need of the case study building.

Since the city center of Perugia is protected by the regulation about preservation of architectural and landscape heritage, the second purpose of this study was to propose a solution for urban landscape requalification of buildings' roofs in historic city centers. In the case study building, in particular, the *Cool-Green roof* is used to recover the flat current concrete roof. This solution improves the roof aesthetic value simultaneously to its environmental sustainability and thermal-energy performance. Furthermore, it may

contribute to the mitigation of Urban Heat Island effect in dense historic city centers, typical of the Italian, and international in general, urban context. Therefore, the results of this study contribute to a further research on the urban application of *Cool-Green roofs* to investigate their potential in improving urban climate conditions and CO_2 offset in city centers. Additionally, the proposed solution could be considered as an effective and non-impactive strategy (i) to mitigate urban heat island in historic city centers subject to rigid urban constraints, and (ii) to preserve architectural heritage, where other common solutions (e.g. urban vegetation, cool paving) are very difficult to be installed.

ACKNOWLEDGMENTS

The authors would like to thank the AIPT (Italian Association Thermo-physical Properties) for rewarding this study with the *"Ermanno Grinzato" award for young researchers in the field of thermo-physical properties* during the *XX Convegno AIPT*, Terni, Italy, September 26th 2014. The first author acknowledgments are due to the "CIRIAF program for UNESCO" in the framework of the UNESCO Chair "Water Resources Management and Culture", for supporting her research.

NOMENCLATURE

Latin symbols

T_{out} outdoor dry bulb temperature [°C]
T_{op} indoor operative temperature [°C]
$T_S(t)$ soil surface temperature [K]
$T_f(t)$ foliage surface temperature of the selected *Helichrysum Italicum* [K]
$H_f(t)$ and $H_S(t)$ sensible heat of the foliage and of the soil, respectively [W/m^2]
$L_f(t)$ and $L_S(t)$ latent heat of the foliage and of the soil, respectively [W/m^2]
$I_f^s(t)$ and $I_f^l(t)$ short wavelength and long wavelength solar radiation, respectively, for the foliage [W/m^2]
$I_S^s(t)$ and $I_S^l(t)$ short wavelength and long wavelength solar radiation, respectively, for the soil [W/m^2]
e_0 windless exchange coefficient, equal to zero in EnergyPlus model [-]
$C_{p\text{-}a}$ specific heat of air at constant pressure [J/kgK]
C_f bulk transfer coefficient [-]
$W_{a\text{-}f}(t)$ foliage wind speed [m/s]
$T_{a\text{-}f}(t)$ air temperature within the foliage layer [K]
C_h^s bulk transfer coefficient for the sensible heat [-]
$I_f(\lambda,t)$ solar spectral irradiance at the foliage surface [W/m^{2}nm]
$I_f^s(t)$ and $I_f^l(t)$ solar spectral irradiance at the foliage surface for the short waves and the long waves, respectively [W/m^{2}nm]
$B(\lambda)$ Plank function: spectral radiant emittance distribution of a black body at the same temperature as the leaf surface [W/m^{2}nm^{-1}]

Greek and composite symbols

α_f and α_s albedo of the foliage and of the soil, respectively [-]
ε_S soil thermal emittance [-]
ε_f foliage thermal emittance of the selected *Helichrysum Italicum* [-]
$\rho_{a\text{-}f}$ *a*ir density within the foliage layer [kg/m^3]
$\rho_{a\text{-}s}$ *a*ir density in correspondence to the soil [kg/m^3]
σ Stefan-Boltzmann constant ($5.6710 \cdot 10^{-8}$ W/m^{2}K^4)
σ_f density of the foliage or foliage fractional coverage, i.e. the ratio of shaded soil to total soil area [-]
$\tau_f(\lambda)$ spectral transmittance of the foliage [-]
τ_f^s and τ_f^l spectral transmittance of the foliage for the short waves and the long waves, respectively [-]

$\rho_f(\lambda)$ spectral reflectance of the foliage [-]
ρ_f^s and ρ_f^l spectral reflectance of the foliage for the short waves and the long waves, respectively [-]
$\varepsilon_f(\lambda)$ and ε_f^l spectral emittance of the foliage total and for the long waves, respectively [-]

REFERENCES

3encult, 2013. Summary Guide for Local Decision Technical guidance on energy efficient renovation of historic buildings. European commission - DG Research and Innovation. Seventh Framework Programme. Grant agreement No. 260162. Available from: http://www.3encult.eu/en/deliverables/Documents/WP3_D3.6_20130527_P21_Technical_guide_EE_options_for_local_governments.pdf

Aeronautica Militare Italiana, 2014. Atlante Climatico 1971-2000, Tabelle climatiche 1971-2000 della stazione meteorologica di Perugia Sant'Egidio. Available from: http://clima.meteoam.it/AtlanteClimatico/pdf/%28181%29Perugia%20S.Egidio.pdf.

Akbari, H., Bretz, S., Kurn, D.M., Hanford, J., 1997. Peak power and cooling energy savings of high-albedo roofs. Energy and Buildings 25 (2), 117-126.

Akbari, H., Konopacki, S., 2005. Calculating energy-saving potentials of heat-island reduction strategies. Energy Policy 33 (6), 721-756.

Ascione, F., de Rossi, F., Vanoli, G.P., 2011. Energy retrofit of historical buildings: theoretical and experimental investigations for the modelling of reliable performance scenarios. Energy and Buildings 43, 1925-1936.

Ascione, F., Bianco, N., de' Rossi, F., Turni, G., Vanoli, G.P., 2013. Green roofs in European climates. Are effective solutions for the energy savings in air-conditioning? Applied Energy 104, 845-859.

ASHRAE, 2005. ASHRAE's Guideline 14-2002 for measurement of energy and demand savings: how to determine what was really saved by the retrofit. American Society of Heating, Refrigerating and Air-Conditioning Engineers, Atlanta, GA.

ASTM E903-96. Standard Test Method for Solar Absorptance, Reflectance, and Transmittance of Materials Using Integrating Spheres.

ASTM C1371-04a, 2010. Standard Test Method for Determination of Emittance of Materials Near Room Temperature Using Portable Emissometers.

ASTM G173-03, 2012. Standard Tables for Reference Solar Spectral Irradiances: Direct Normal and Hemispherical on 37° Tilted Surface.

Berardi, U., GhaffarianHoseini, Am., GhaffarianHoseini, Al., 2014. State-of-the-art analysis of the environmental benefits of green roofs. Applied Energy 115, 411-428.

Berdahl, P., Bretz, S.E., 1007. Preliminary survey of the solar reflectance of cool roofing materials. Energy and Buildings 25 (2), 149-158.

Deardoff, J.W., 1987. Efficient prediction of ground surface temperature and moisture, with inclusion of a layer of vegetation. Journal of Geophysical Research 96, 541-550.

EN 15251, 2007. Indoor environmental input parameters for design and assessment of energy performance of buildings addressing indoor air quality, thermal environment, lighting and acoustics.

EN ISO 7730, 2005. Ergonomics of the thermal environment – Analytical determination and interpretation of thermal comfort using calculation of the PMV and PPD indices and local thermal comfort criteria.

EN ISO 6946, 2007. Building components and building elements. Thermal resistance and thermal transmittance. Calculation method.

European Parliament and Council of the European Union, 2010. Directive 2010/31/EU of 19 May 2010 on the Energy Performance of Buildings. Official Journal of the European Union. Available from: http://eur- lex.europa.eu/LexUriServ/LexUriServ.do?uri=OJ:L:2010:153:0013:0035:EN:PDF.

Ferrante, A., Mihalakakou, G., 2001. The influence of water, green and selected passive techniques on the rehabilitation of historical industrial buildings in urban areas. Solar Energy 70, 245-253.

French, A.N., Schmugge, T.J., Kustas, W.P., 2000. Discrimination of Senescent Vegetation Using Thermal Emissivity Contrast. Remote Sensing of Environment 74, 249-254.
Hosseini, M., Akbari, H., 2014. Heating energy penalties of cool roofs: the effect of snow accumulation on roofs. Advances in Building Energy Research 8 (1) 1-13.
IEA World Energy Outlook 2008–2009. International Energy Agency, Geneva (2009).
Kolokotsa, D., Maravelaki-Kalaitzaki, P., Papantoniou, S., Vangeloglou, E., Saliari, M., Karlessi, T., Santamouris, M., 2012. Development and analysis of mineral based coatings for buildings and urban structures. Solar Energy 86, 1648–1659.
Kolokotsa, D., Santamouris, M., Zerefos, S.C., 2013. Green and cool roofs' urban heat island mitigation potential in European climates for office buildings under free floating conditions. Solar Energy 95, 118-130.
ISO 9869, 1994. Thermal insulation – Building elements - In-situ measurement of thermal resistance and thermal
transmittance.
Levinson, R., Chen, S., Berdahl, P., Rosado, P., Medina, L.A., 2014. Reflectometer measurement of roofing aggregate albedo. Solar Energy 100, 159-171.
Libbra, A., Tarozzi, L., Muscio, A., Corticelli, M.A., 2011. Spectral response data for development of cool coloured tile coverings. Optics & Laser Technology 43, 394-400.
Lawrence Berkeley National Laboratory, 2000. Cool Roofing Materials Database – Membranes. Available from: http://energy.lbl.gov/coolroof/membrane.htm#membrane.
Ministero per la Pubblica Istruzione, Repubblica Italiana, 1961. D.M. 11 settembre 1961: Dichiarazione di notevole interesse pubblico della zona racchiusa entro l'intera cinta di mura urbiche, sita nell'ambito del comune di Perugia. Gazzetta Ufficiale n. 231 del 19 settembre 1961, Roma, Italy. In italian.
Niachou, A., Papakonstantinou, K., Santamouris, M., Tsangrassoulis, A., Mihalakakou, G., 2001. Analysis of the green roof thermal properties and investigation of its energy performance. Energy and Buildings 33 (7), 719-729.
Ouldboukhitine, S.E., Belarbi, R., Jaffal, I., Trabelsi, A., 2011. Assessment of green roof thermal behavior: A coupled heat and mass transfer model. Building and Environment 46, 2624-2631.
Pandey, S., Hindoliya, D.A., Mod, R., 2013. Experimental investigation on green roofs over buildings. International Journal of Low-Carbon Technologies 8, 37-42.
Paolini, R., Zinzi, M., Poli, T., Carnielo, E., Mainini, A.G., 2014. Effect of ageing on solar spectral reflectance of roofing membranes: Natural exposure in Roma and Milano and the impact on the energy needs of commercial buildings. Energy and Buildings 84, 333-343.
Pisello, A.L., Goretti, M., Cotana, F., 2012. A method for assessing buildings' energy efficiency by dynamic simulation and experimental activity. Applied Energy 97, 419-429.
Pisello, A.L., Cotana, F., Nicolini, A., Brinchi, L., 2013. Development of clay tile coatings for steep-sloped cool roofs. Energies 6, 3637-3653.
Pisello, A.L., Cotana, F., Nicolini, A., Buratti, C., 2014a. Effect of dynamic characteristics of building envelope on thermal-energy performance in winter conditions: In field experiment. Energy and Buildings 80, 218-230.
Pisello, A.L., Rossi, F., Cotana, F., 2014b. Summer and winter effect of innovative cool roof tiles on the dynamic thermal behavior of buildings. Energies 7 (4), 2343-2361.
Presidente della Repubblica, Repubblica Italiana, 2004. D.Lgs. n.42 22 gennaio 2004: Codice dei beni culturali e del paesaggio, ai sensi dell'articolo 10 della legge 6 luglio 2002, n. 137. Gazzetta Ufficiale n. 45 del 24 febbraio 2004 - Supplemento Ordinario n. 28, Roma, Italy.
Regione Umbria, 2012. Piano Paesaggistico Regionale – Volume 1: Per una maggiore consapevolezza del valore del paesaggio – Relazione illustrativa, Perugia, Italy. In italian.
Revel, G.M., Martarelli, M., Emiliani, M., Celotti, L., Nadalini, R., De Ferrari, A., Hermanns, S., Beckers, E., 2014. Cool products for building envelope - Part II: Experimental and numerical evaluation of thermal performances. Solar Energy 105, 780-791.

Sailor, D.J., Hutchinson, D., Bokovoy, L., 2008. Thermal property measurements for ecoroof soils common in the western U.S. Energy and Buildings 40 (7), 1246-1251.

Salata, F., De Lieto Vollaro, A., Ferraro, A., 2014a. An economic perspective on the reliability of lighting systems in building with highly efficient energy: A case study. Energy Conversion and Management 84, 623-632.

Salata, F., De Lieto Vollaro, A., De Lieto Vollaro, R., 2014b. A case study of technical and economic comparison among energy production systems in a complex of historic buildings in Rome. Energy Procedia 45, 482-491.

Santamouris, M., Synnefa, A., Karlessi, T., 2011. Using advanced cool materials in the urban built environment to mitigate heat islands and improve thermal comfort conditions. Solar Energy 85, 3085-3102.

Santamouris, M., 2014. Cooling the cities – A review of reflective and green roof mitigation technologies to fight heat island and improve comfort in urban environments. Solar Energy 103, 682-703.

Scurlock, J.M.O., Asner, G.P., Gower, S.T., 2001. Worldwide Historical Estimates of Leaf Area Index, 1932-2000. Oak Ridge National Laboratory, Oak Ridge, Tennessee.

Takebayashi, H., Moriyama, M., 2012. Relationships between the properties of an urban street canyon and its radiant environment: Introduction of appropriate urban heat island mitigation technologies. Solar Energy 86, 2255-2262.

Taleghani, M., Tenpierik, M., van den Dobbelsteen, A., Sailor, D.J., 2014. Heat in courtyards: A validated and calibrated parametric study of heat mitigation strategies for urban courtyards in the Netherlands. Solar Energy 103, 108-124.

U.S. Department of Energy, Energy Efficiency and Renewable Energy, 2014a. Building technologies program: EnergyPlus.

U.S. Department of Energy, Energy Efficiency and Renewable Energy, 2014b. Available from: http://apps1.eere.energy.gov/buildings/energyplus/cfm/weather_data3.cfm/region=6_europe_wmo_region_6/country=ITA/cname=Italy, WMO Station Region 6: Italy, Perugia 161810 (IGDG).

Voltolina, G., 2001. Elicriso (Helichrysum Italicum (Roth) Don.), Piante officinali, Schede di divulgazione Veneto Agricoltura. Available from: http://www.pianteofficinali.org/main/Schede/Elicriso.pdf.

Zinzi, M., Agnoli, S., 2012. Cool and green roofs. An energy and comfort comparison between passive cooling and mitigation urban heat island techniques for residential buildings in the Mediterranean region. Energy and Buildings 55, 66-76.

Zinzi, M., Carnielo, E., Federici, A. 2014. Preliminary studies of a cool roofs' energy-rating system in Italy. Advances in Building Energy Research 8 (1), 84-96.

HIGHLIGHTS

- An innovative type of green roof, i.e. *Cool-Green roof (CGR)*, is proposed
- The CGR analytic and numerical year-round thermal-energy performance is assessed
- Calibrated dynamic simulation of a historic case-study building is performed
- The CGR dampens down the indoor temperature in summer with limited winter penalties
- The *CGR* is a low impact strategy for energy retrofitting and UHI mitigation

Graphical Abstract (for review)

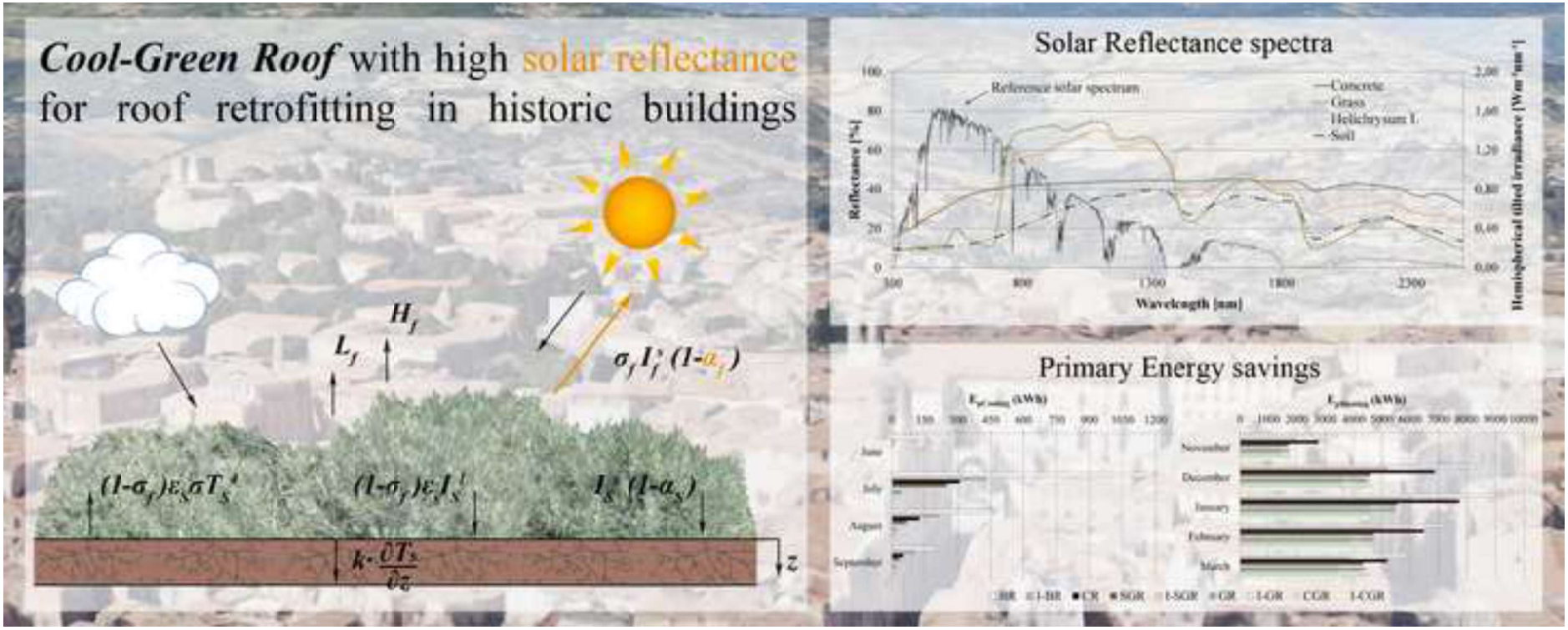

THERMAL-PHYSICS AND ENERGY PERFORMANCE OF AN INNOVATIVE GREEN ROOF SYSTEM: THE COOL-GREEN ROOF

Anna Laura Pisello[a,*], Cristina Piselli[a], Franco Cotana[a]

[a] Department of Engineering – University of Perugia, Via Duranti 67, 06125, Perugia, Italy

Tel. +39 075 585 3563, Email: *pisello@crbnet.it; piselli@crbnet.it; cotana@crbnet.it

TABLES and CAPTIONS (REVISED VERSION)

Table 1. Technical features of spectrophotometer and emissometer.

Spectrophotometer *Shimadzu SolidSpec 3700*	
Spectral bandwidth	UV/VIS: 0,1-8 nm (8 steps) NIR: 0,2-32 nm (10 steps)
Spectrum interval	240÷2600 nm
Resolution	0,1 nm
Wavelength accurancy	UV/VIS: ±0,2 nm NIR: ±0,8 nm
Wavelength repeatability	UV/VIS: ±0,08 nm NIR: ±0,32 nm
IR resolution	320 x 240
Noise	<0,0002 Abs (500 nm, SBW 8 nm) <0,00005 Abs (1500 nm, SBW 8 nm) determined under conditions of RMS value at 0Abs and 1s response
Photometric range	-6 to 6 Abs
Accurancy	±2% of reading
Emissometer *AE1 RD1*	
Repeatability	±0,01 emittance units
Total hemispherical emittance approximation	at 65 °C
Linearity	±0,01 units
Time costant	10 sec
Max sample temperature	54 °C
Measuring head dimensions	5,7 cm across
Output	2,4 millivolts with sample emittance of 0,9 and temperature of 25 °C
Heat flowmeter plate *Ahlborn* *Heat Flow Plates FQA 150-2*	
Dimensions	500 × 500 × 6 (mm)
Meander Size	490 × 490 (mm)
Substrate	PTFE
Temperature Stability	150°C
Calibr. Val. appr. (W/m2 ≈ mV)	<10
Accuracy of calibration value	5% at 25°C
Nominal temperature	23 °C
Temperature coefficient	-0.12 % / K (epoxide plate)

Table 2. Technical data of the case study building.

Building Location data	Perugia, Italy Lat. 43°06'34.9"N Long. 12°23'14.7"E Altitude: 472 a.s.l. Italian Climatological classification: Class E (2289 degree days)
Building architectural features	
Internal conditioned area	172 m^2
Transparent envelope properties	Double glazing system 4 mm - 6mm (air) - 4 mm Solar Heat Gain Coefficient: 0.80 [-] U (ISO10292/EN673): 2.76 W/m^2K
Opaque envelope properties	**Layer materials** (from outside to inside)
External wall – typology 1	1. Sedimentary rock: 1.10 m 2. Plaster Dense: 0.04 m 3. Gypsum Plaster: 0.01 m
Measured Thermal Transmittance = 1.2 W/m^2K	
Internal Heat Capacity = 190.1 kJ/m^2K	
External wall – typology2	1. Plaster Dense: 0.02 m 2. Brickwork (Outer leaf): 0.15 m 3. Gypsum Plaster: 0.01 m
Measured Thermal Transmittance = 2.3 W/m^2K	
Internal Heat Capacity = 155 kJ/m^2K	
External wall – typology 3	1. Sedimentary rock mixed to brickworks: 0.30 m 2. Plaster Dense: 0.03 m 3. Gypsum Plaster: 0.01 m
Measured Thermal Transmittance = 2.6 W/m^2K	
Internal Heat Capacity = 148 kJ/m^2K	
Window systems	
Double-Glass camera	3 mm – 6 mm Air – 3 mm
	Total solar transmission SHGC: 0.76 Direct solar transmission: 0.71 Light transmission: 0.81 U-value: 3.23 W/m^2K
Wood frame (thickness: 40 mm)	Painted wood window frame U-value: 2.63 W/m^2K
Occupancy level	Non-occupied - 0 W/m^2
Air conditioning technologies	Free floating conditions – non operative HVAC system

Table 3. Principal monthly characteristics of the weather conditions of the considered site.

Monthly Statistics for Dry bulb Temperature (°C)												
	Jan	Feb	Mar	Apr	May	Jun	Jul	Aug	Sep	Oct	Nov	Dec
Max	12.6	15	17.4	20	26.2	29.8	34.3	34.1	29.8	24	17.3	12.9
Min	-3.7	-6	-1	3.1	7.6	8.6	12.6	13.8	9.4	5.8	-0.6	-1
Ave	4.3	5.4	7.3	11	15.4	19.5	22.3	22.1	18.5	13.5	9.5	5.3
Monthly Solar Irradiance (noon on 21st of month) (Wh/m²)												
I_{beam} [a]	789	809	820	835	840	820	811	798	800	765	714	740
$I_{diffuse}$ [b]	95	129	160	175	172	177	174	167	142	126	110	90

[a] Clear Sky Noon Beam Normal Irradiance on 21st Day

[b] Clear Sky Noon Diffuse Horizontal Irradiance on 21st Day

Table 4. Green roof properties.

Scenario	Growing media (m)	Average Plants height (m)	LAI
Green Roof	0.30	0.10	1.5
Cool-Green Roof	*0.30*	*0.25*	*3.0*
Soil-Green Roof	0.30	0.02	0.002

Table 5. Solar Reflectance and Thermal Emittance properties of the different materials.

Sample	R_{uv} (%)	R_{vis} (%)	R_{nir} (%)	R_{solar} (%)	Emittance ε^{l}
Concrete	18.7	34.2	43.1	37.5±2.2	0.88
Grass	9.3	19.5	61.1	36.9±2.0	0.98
Soil	9.4	12.5	30.2	19.9±0.9	0.93
Helichrysum It.	*19.4*	*35.3*	*56.7*	*43.9±2.7*	*0.98*
Bitumen membrane[2]	-	-	-	6.0	0.86

1. values refers to French et al., 2000
2. Lawrence Berkeley National Laboratory, 2000.

Table 6. MBE and RMSE values before and after the calibration process.

		MBE (°C)	RMSE (°C)
Initial model	ER	-2.78	4.21
	SR	-4.81	5.67
Iterative procedure			
Calibrated model	*ER*	*0.17*	*0.82*
	SR	*0.02*	*0.79*

Table 7. Number of hours with temperature higher than 26°C in summer.

	CR	BR	I-BR	GR	I-GR	CGR	I-CGR
	Number of hours when T>26°C from April to September						
T Air	943	1992	1467	269	202	61	55
T Mean Rad	1010	2077	1517	277	153	3	0
T Operative	952	2044	1483	259	175	17	19
	Percentage increase/decrease of T>26°C hours						
T Air	-	+111.2%	+55.6%	-71.5%	-78.6%	-93.5%	-94.2%
T Mean Rad	-	+105.6%	+50.2%	-72.6%	-84.9%	-99.7%	-100.0%
T Operative	-	+114.7%	+55.8%	-72.8%	-81.6%	-98.2%	-98.0%

Table 8. Number of hours with temperature lower than 20°C in winter.

	CR	BR	I-BR	GR	I-GR	CGR	I-CGR	SGR	I-SGR
	Number of hours when T<20°C from October to March								
T Air	4097	4095	4006	4027	3993	4058	4001	4012	3969
T Mean Rad	4087	4084	4002	4014	3983	4043	3989	4011	3976
T Operative	4095	4090	4006	4015	3987	4050	3998	4011	3982
	Percentage decrease of T<20°C hours compared to CR								
T Air	-	-0.1%	-2.3%	-1.7%	-2.6%	-1.0%	-2.4%	-2.1%	-3.2%
T Mean Rad	-	-0.1%	-2.1%	-1.8%	-2.6%	-1.1%	-2.5%	-1.9%	-2.8%
T Operative	-	-0.1%	-2.1%	-2.0%	-2.7%	-1.1%	-2.4%	-2,1%	-2.8%
	Percentage increase of T<20°C hours compared to SGR and I-SGR								
T Air	-	-	-	+0.4%	+0.6%	+1.1%	+0.8%	-	-
T Mean Rad	-	-	-	+0.1%	+0.2%	+0.8%	+0.3%	-	-
T Operative	-	-	-	+0.1%	+0.1%	+1.0%	+0.4%	-	-

Table 9. Fanger's and Adaptive Thermal Comfort model results for the different scenarios.

FANGER MODEL	**Winter**			**Summer**		
	% hours of overcooling	% hours of overheating	PPD (%)	% hours of overheating	% hours of overcooling	PPD (%)
CR	100	0	81	23	17	13
BR	100	0	81	66	5	23
I-BR	100	0	76	44	11	15
GR	100	0	76	3	23	12
I-GR	97	0	72	1	24	12
CGR	*100*	*0*	*76*	*0*	*31*	*14*
I-CGR	*100*	*0*	*73*	*0*	*29*	*13*
SGR	100	0	76	-	-	-
I-SGR	97	0	72	-	-	-
ADAPTIVE MODEL	**Winter**			**Summer**		
	% hours of overcooling	% hours of overheating	Degree Hours	% hours of overheating	% hours of overcooling	Degree Hours
CR	100	0	31880	0	9	1151
BR	100	0	32273	17	0	4319
I-BR	100	0	28631	0	6	1906
GR	100	0	28451	0	15	115
I-GR	100	0	26640	0	16	72
CGR	*100*	*0*	*28929*	*0*	*20*	*12*
I-CGR	*100*	*0*	*27436*	*0*	*21*	*10*
SGR	100	0	28456	-	-	-
I-SGR	100	0	26631	-	-	-

Table 10. Annual primary energy requirements.

	E_p annual (kWh)	% increase/decrease compared to CR
CR	29542.6	-
BR	36036.3	+22%
I-BR	22751.9	-23%
GR	20858.3	-29%
I-GR	16772.0	-43%
CGR (1)	21492.4	-27%
I-CGR (3)	17169.2	-42%
SGR (2)	21216.2	-28%
I-SGR (4)	17031.0	-42%
Comb. (1)+(2)	20875.8	-29%
Comb. (3)+(4)	16800.6	-43%

THERMAL-PHYSICS ASSESSMENT OF INNOVATIVE ROOF SYSTEMS FOR APPLICATION IN HISTORIC BUILDINGS

Anna Laura Pisello[a,*], Cristina Piselli[a], Franco Cotana[a]

[a] Department of Engineering – University of Perugia, Via Duranti 67, 06125, Perugia, Italy

Tel. +39 075 585 3563, Email: *pisello@crbnet.it; piselli@crbnet.it; cotana@crbnet.it

FIGURES CAPTIONS (REVISED VERSION)

Fig. 1. Examples of horizontal roofs in the historical city center misuse in Perugia, Italy, and case study roof in central Italy (*).

Fig. 2. *Helichrysum Italicum* ("Curry plant") used in this study: (a) foliage, (b) paving installation, (c) plant used for the sample development.

Fig. 3. Different fluxes participating to the green roof energy balance.

Fig. 4. (a) Spectrophotometer, and (b) emissometer and heat flowmeter apparatus instruments for the in-lab and in-field experimental analysis.

Fig. 5. (a) Building façade, (b) living room and (c) top floor plan.

Fig. 6. (a) Solar reflectance of the various samples and the solar spectrum; (b) thermal transmittance of opaque wall typologies.

Fig. 7. Measured and simulated indoor temperatures for ER and SR.

Fig. 8. Attic operative temperature hourly trends for the different scenarios.

Fig. 9. PMV and PPD indexes for the different scenarios.

Fig. 10. TDI indexes for the different scenarios.

Fig. 11. Primary energy requirement (a) for cooling and (b) for heating.

Figure 1

Click here to download high resolution image

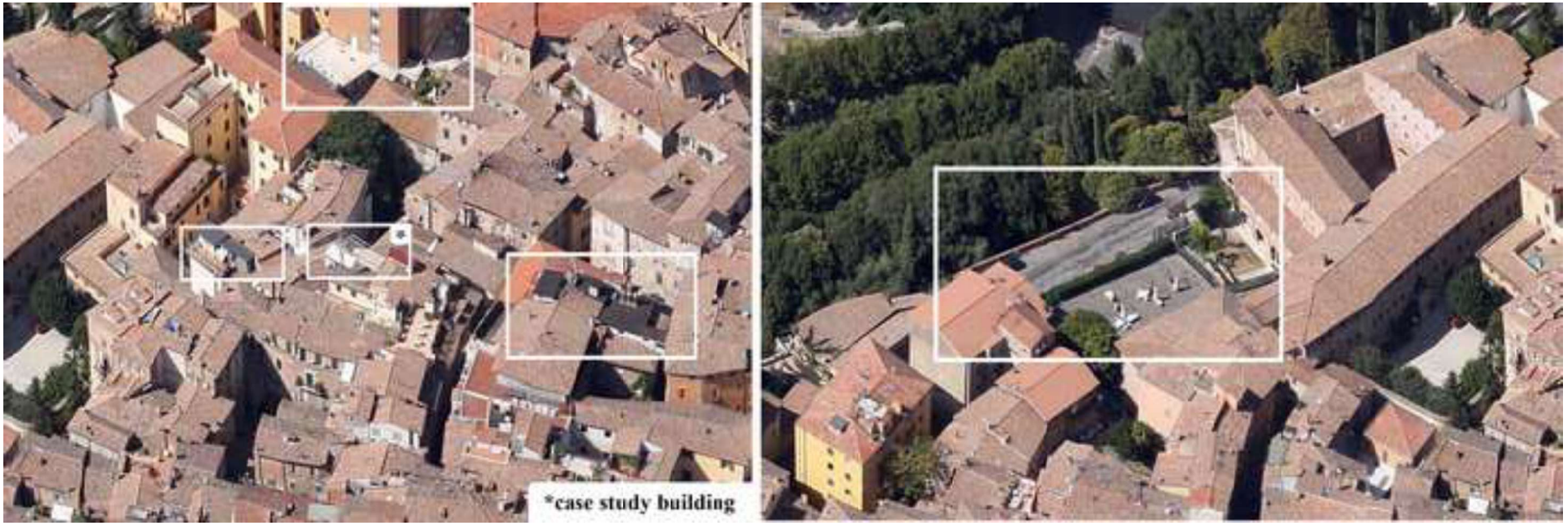

Figure 2

Click here to download high resolution image

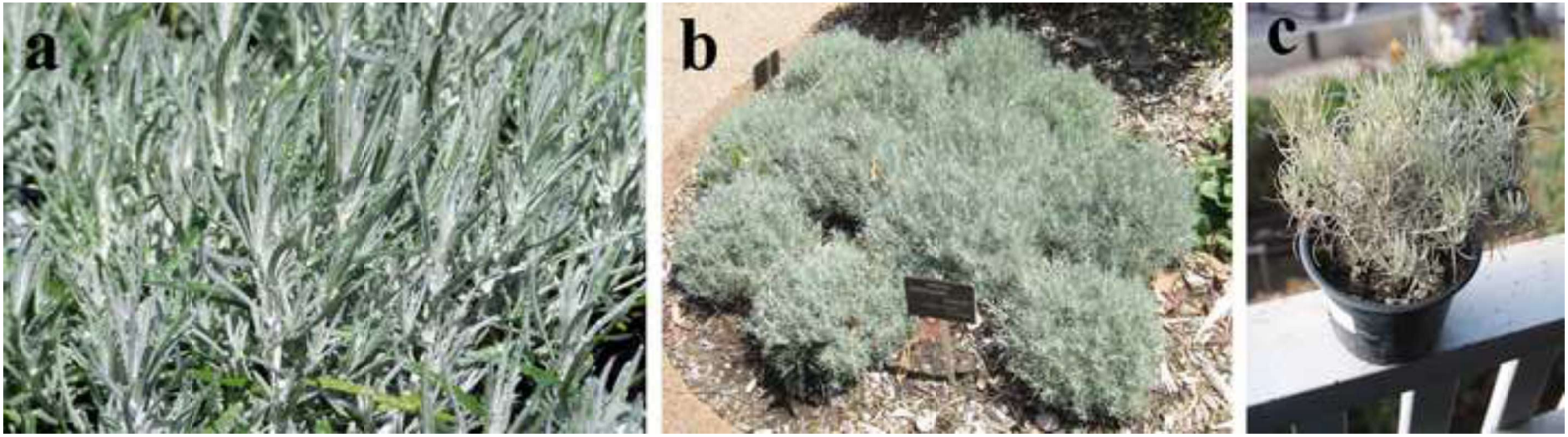

Figure 3

Click here to download high resolution image

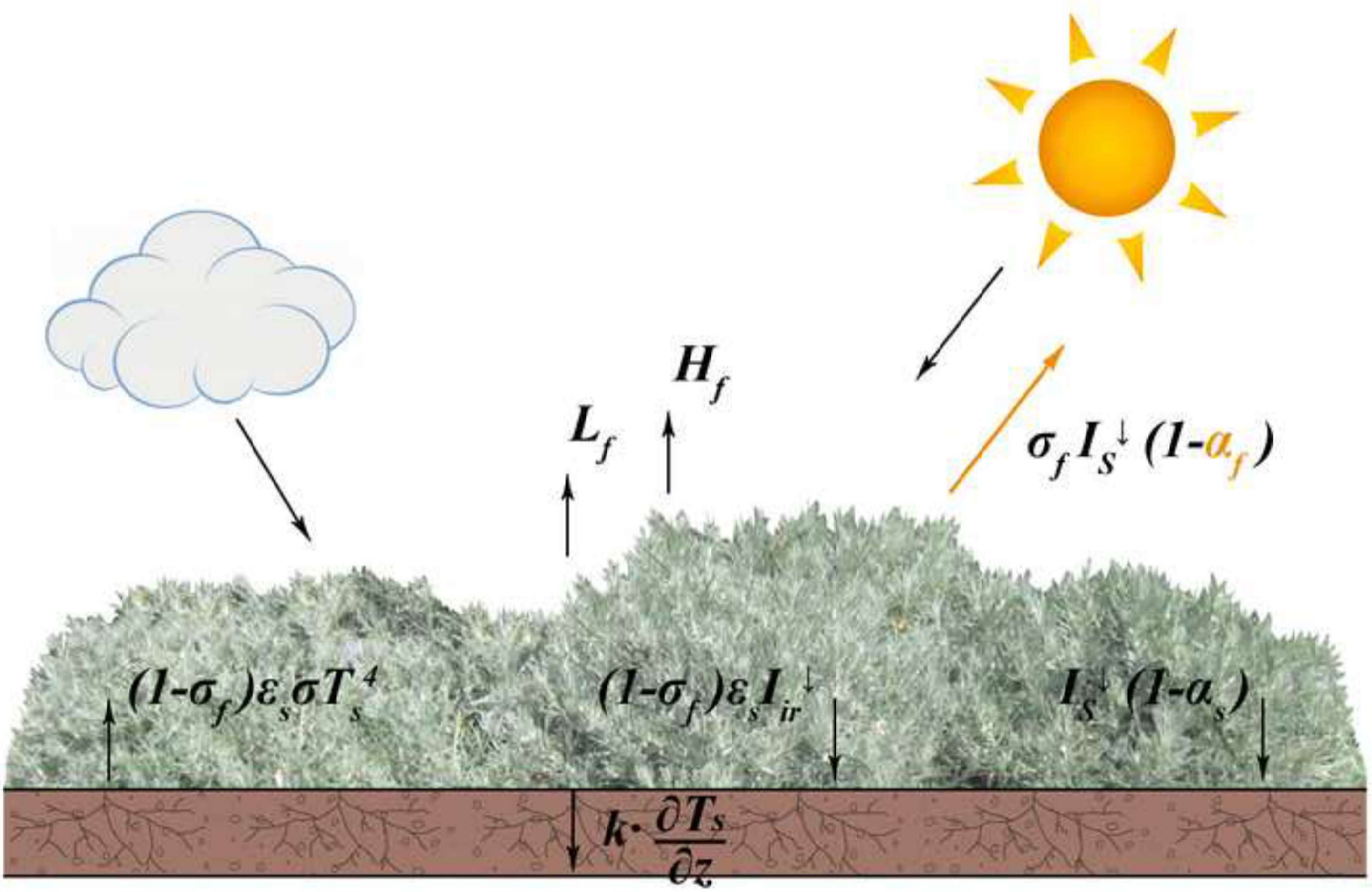

Figure 4 rev

Click here to download high resolution image

Figure 5 rev
Click here to download high resolution image

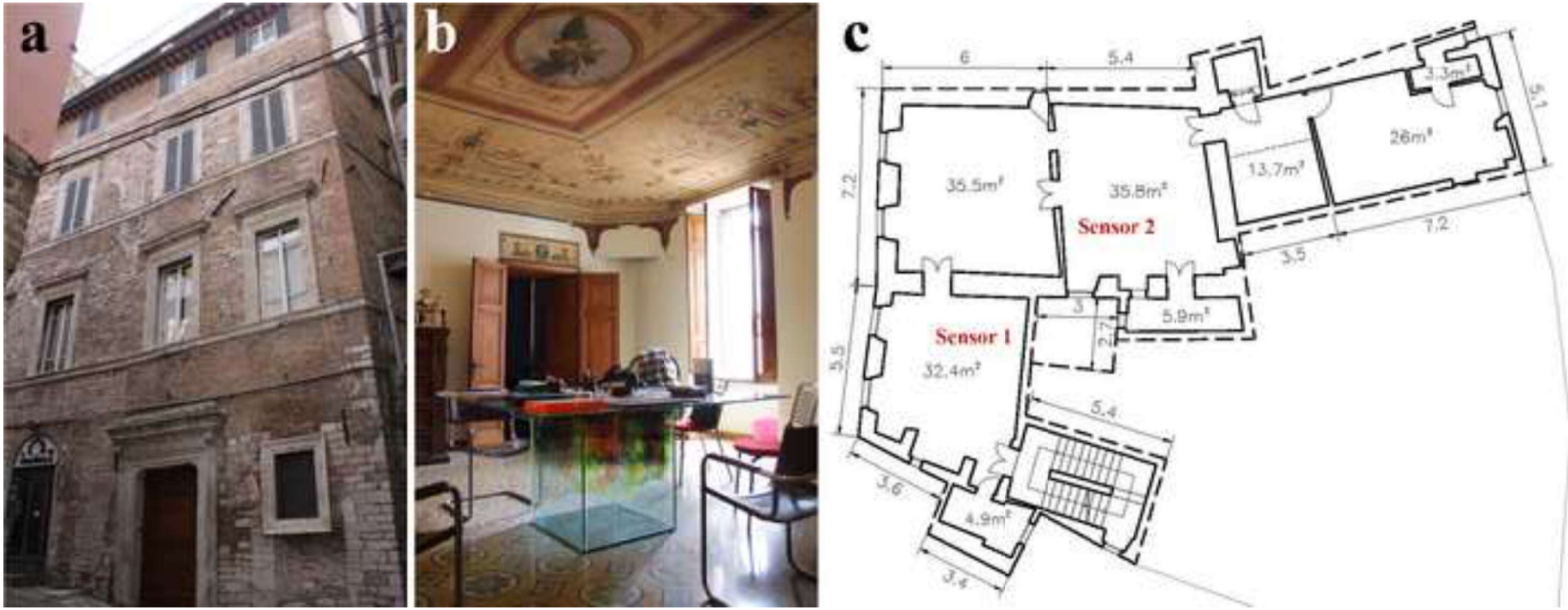

Figure 8 rev

Click here to download high resolution image

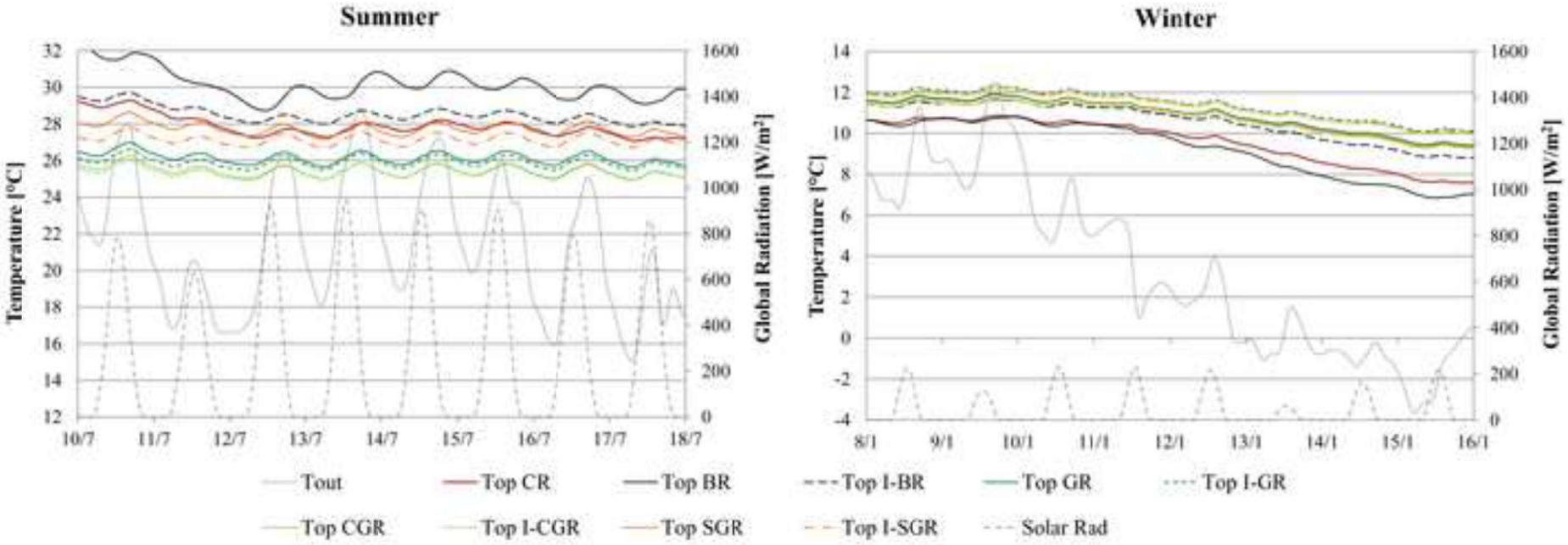

Figure 9 rev

Click here to download high resolution image

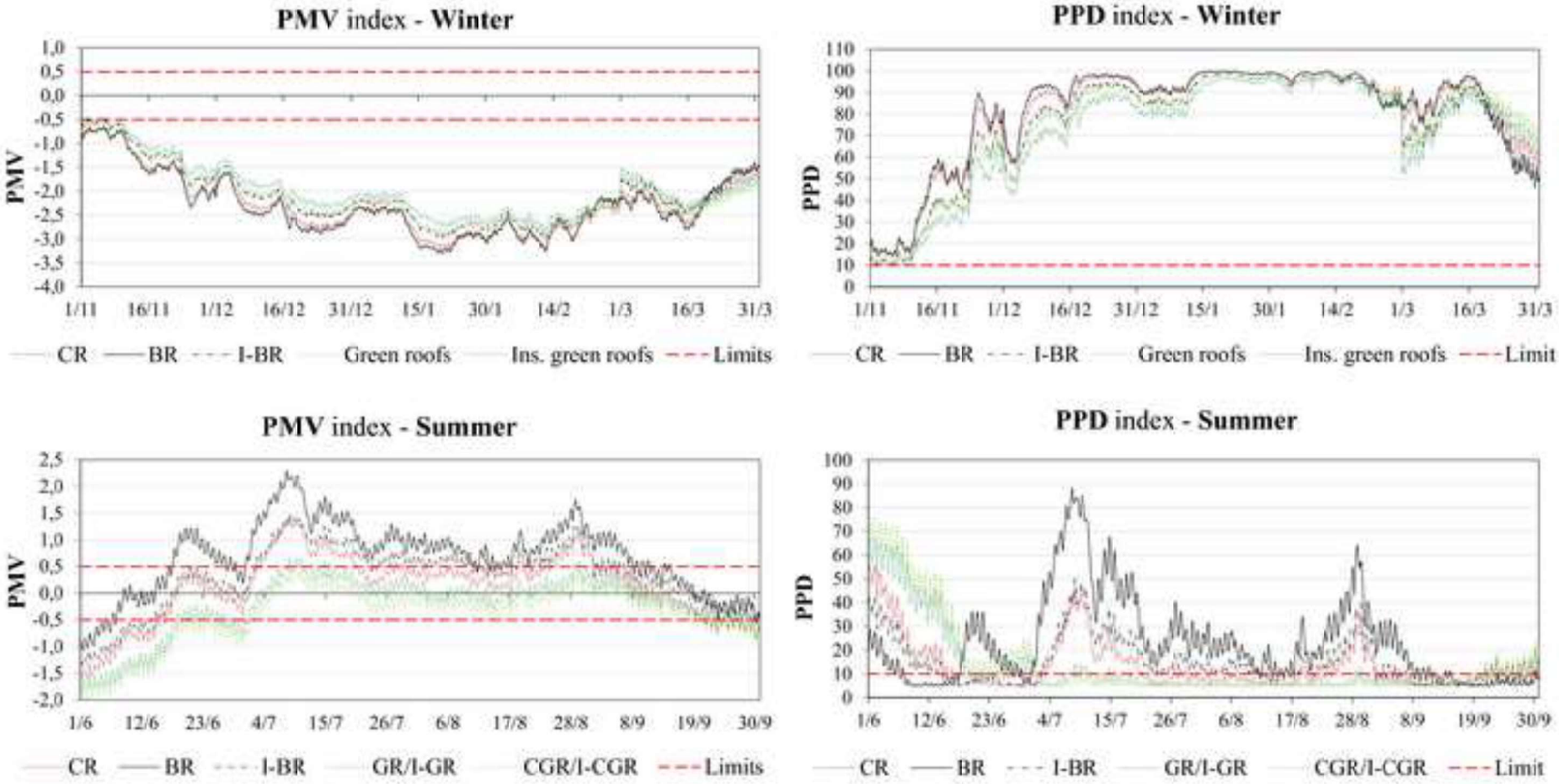

Figure 10 rev

Click here to download high resolution image

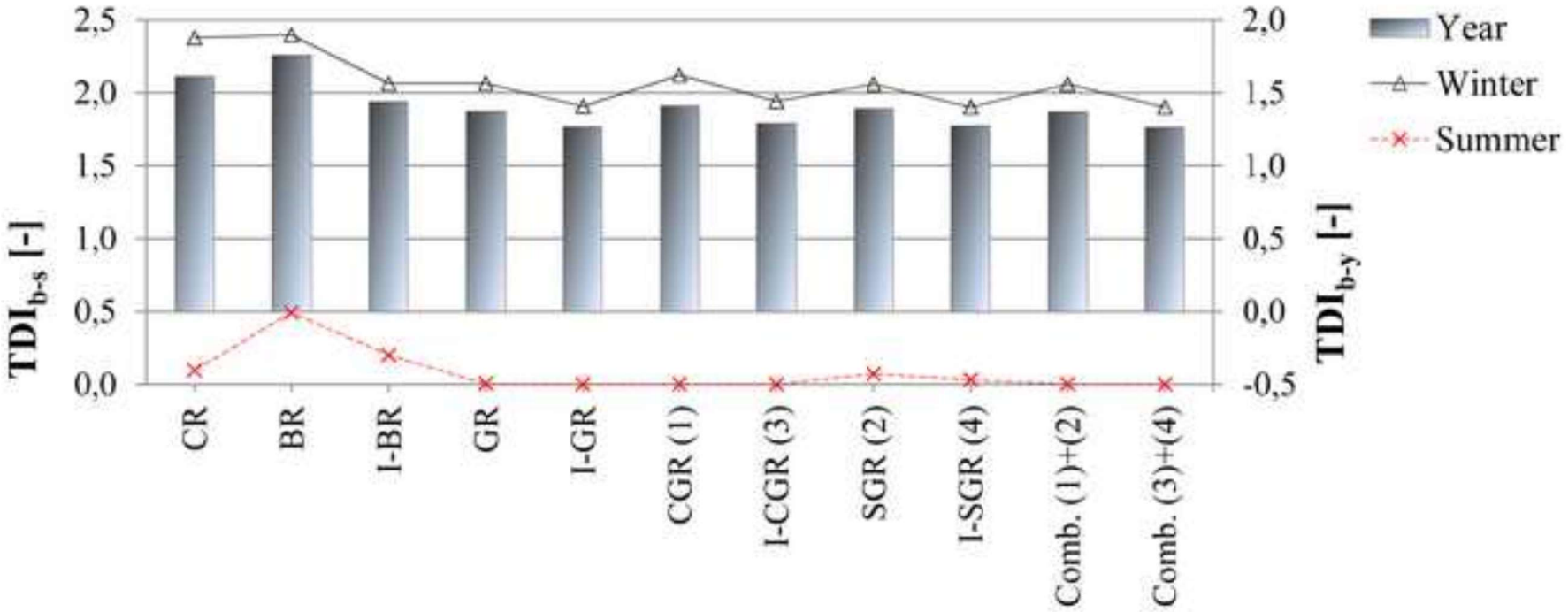

Figure 11 rev

Click here to download high resolution image

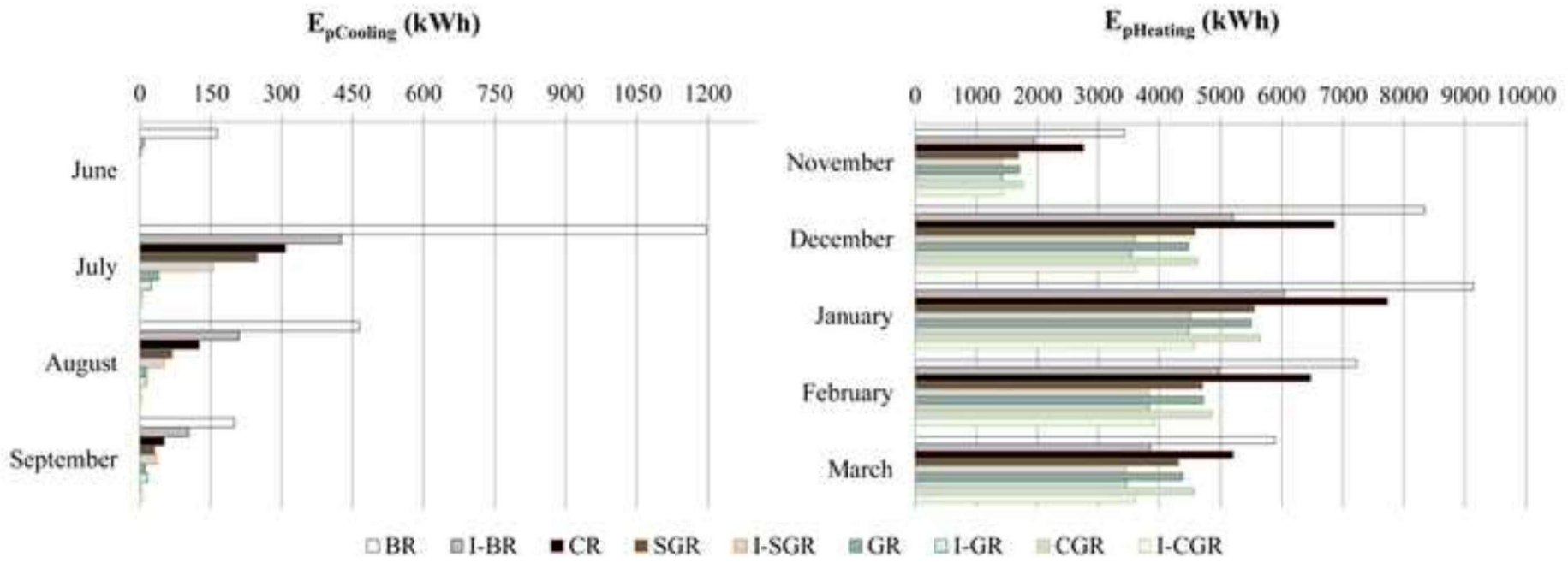

Figure 6 rev

Click here to download high resolution image